IEEE SENSORS 2013
Tutorials: November 3, 2013 Conference: November 4-6, 2013
Sponsored by the IEEE Sensors Council, www.ieee-sensors.org

Design and Analysis of MEMS Gyroscopes

Diego Emilio Serrano
Qualtré
Georgia Institute of Technology

What is a Gyroscope?

- Sensor that measures the angle or rate of rotation

Spinning Gyroscopes

Conservation of angular momentum

Optical Gyroscopes

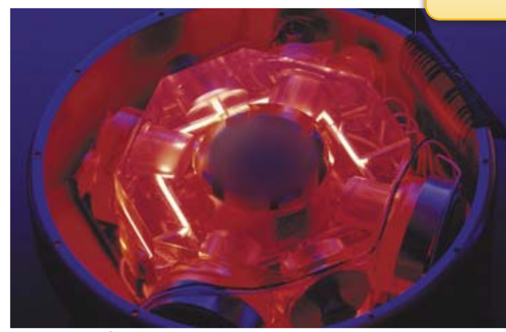

Sagem's RLG

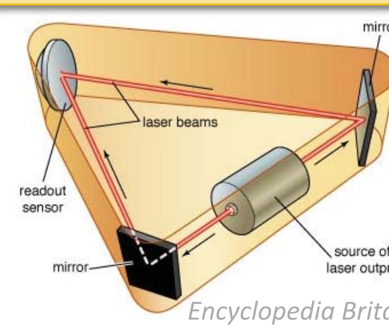

Encyclopedia Britannica

Sagnac Effect

Vibratory Gyroscopes

Northrop Grumman HRG

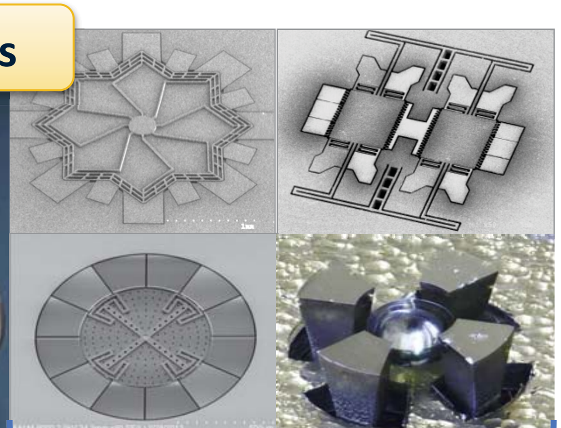

Coriolis Effect

MEMS

NMR Gyroscopes

Northrop Grumman NMR Gyro

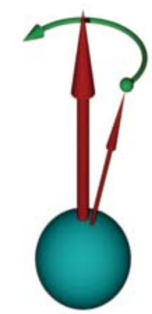

Larmor Precession Rate

Applications of MEMS Gyroscopes

Automotive: Reliability

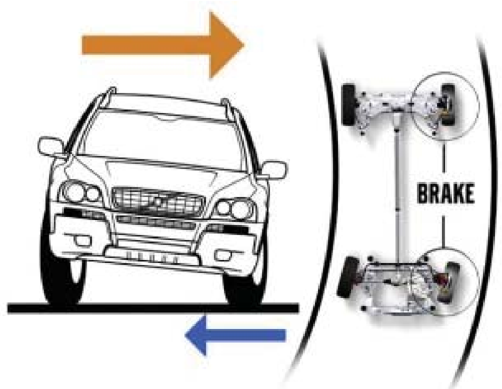

Anti-skid control

Industrial: Robustness

Antenna stabilization

Precision machinery

Consumer: Size & Cost

Gaming

Health and fitness

Optical Image Stabilization

Pedestrian Navigation

Evolution of MEMS Gyroscopes

- STMicroelectronics 3-Axis Gyroscope (Consumer)

(2009)

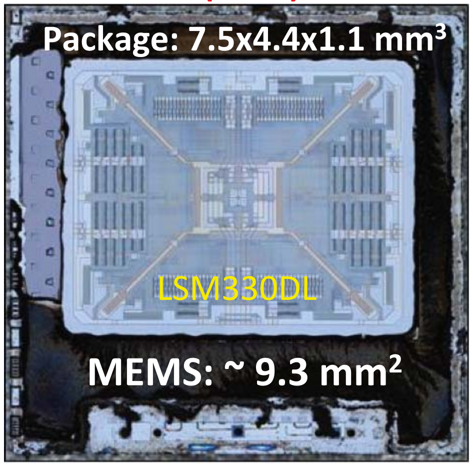

(2010)

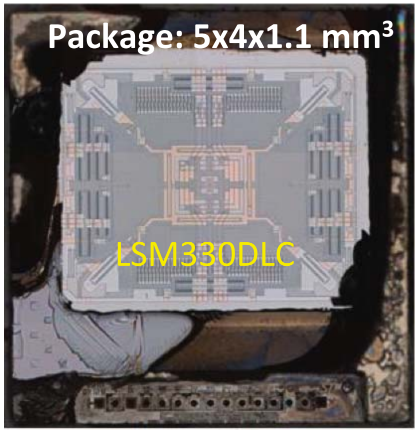

(2011)

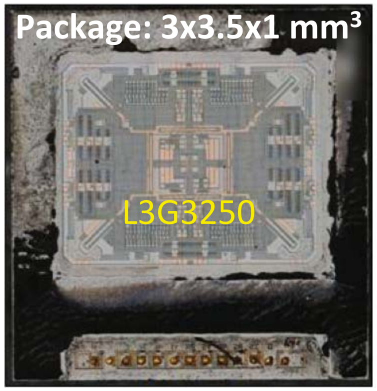

(2013)

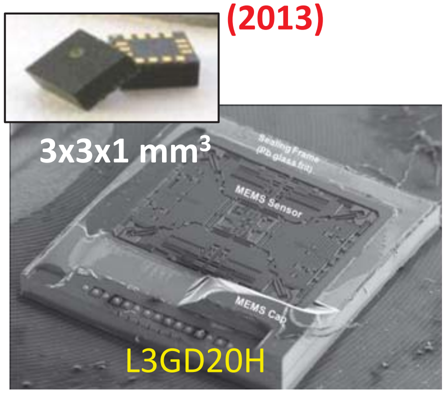

Source: Yole Développement, "STMicro L3G3250A Reverse costing", 2012

- Invensense 3-Axis Gyroscope (Commercial)

Product	IDG-1000	IDG-600	IXZ-600	MPU-3000	
MP Date	2006	2008	2009	2010	
Gyro Axes	X/Y	X/Y	X/Z	X/Y/Z	
Package	6x6x1.4 QFN	5x4x1.2 QFN	5x4x1.2 QFN	4x4x0.9 QFN	mm^3
Die Size	12.2	7.4	7.4	6.7	mm^2
MEMS Area	4.1	2.8	2.8	2.9	mm^2
CMOS technology	0.5um	0.35um	0.35um	0.18um	
Output	Analog	Analog	Analog	Digital	

(2012)

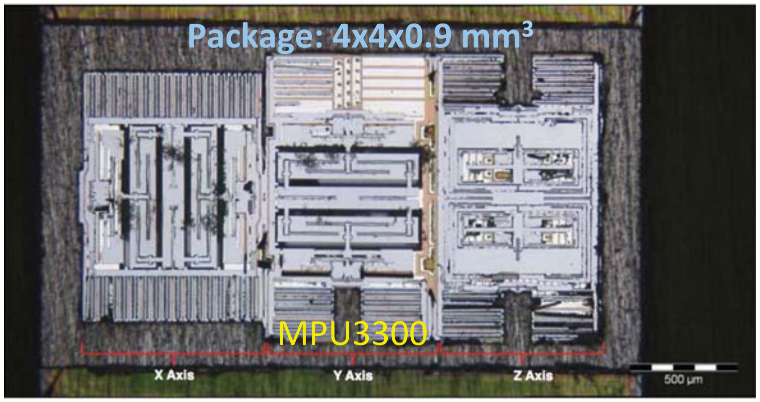

Source: Seeger, et. al. "Development of High-Performance, High-Volume Consumer MEMS Gyroscopes." *Solid-State Sensor, Actuator and Microsystems Workshop, Hilton Head Island*. 2010.

Performance in Gyroscopes (Consumer)

- Current applications do not demand low-noise performance
- Pedestrian and in-doors navigation → LOW NOISE IS A MUST!

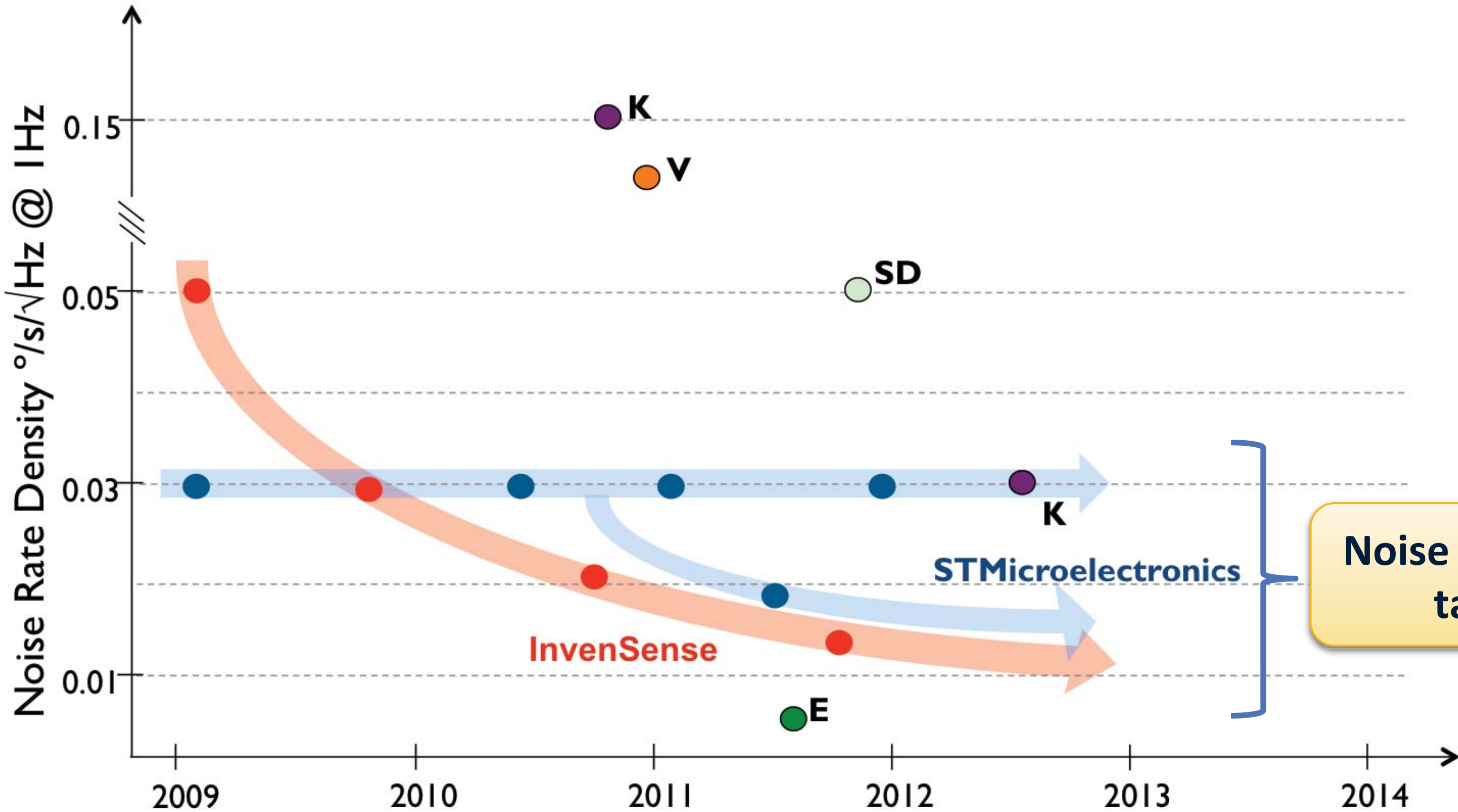

Noise performance tapering?

Is it time for a new technology?

Operation Principles - The Coriolis Effect

- Example: The Foucault Pendulum

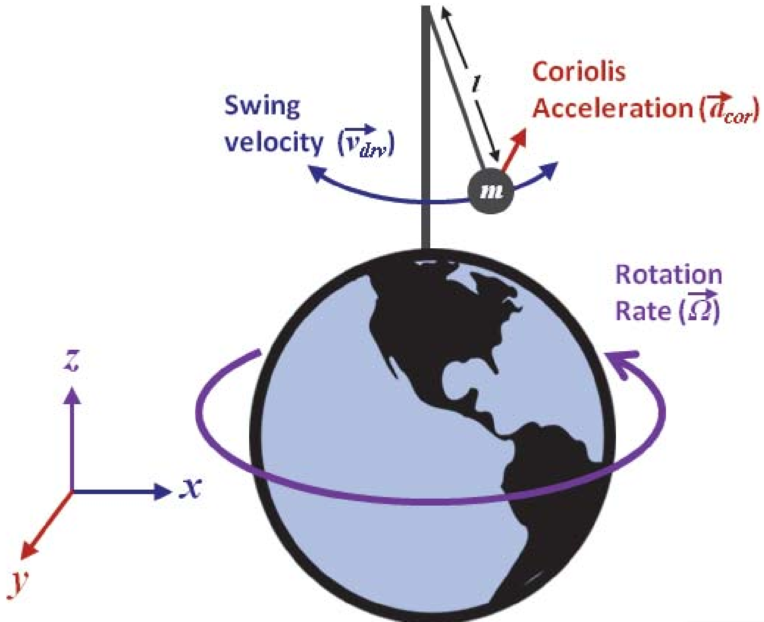

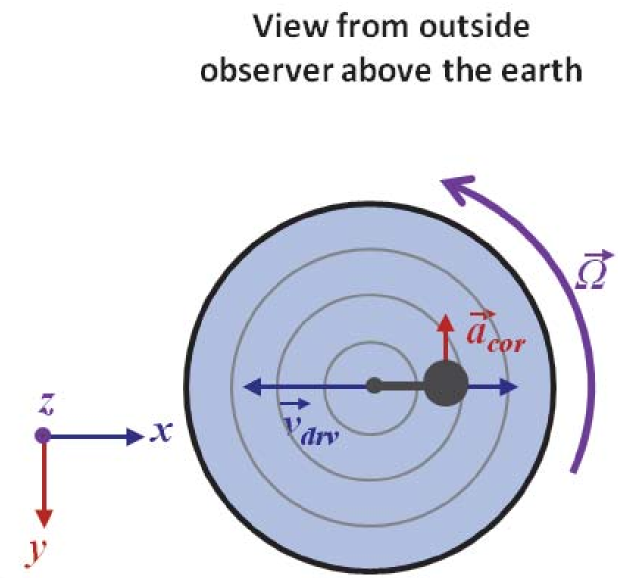

$$\vec{a}_{cor} = -2\vec{\Omega} \times \vec{v}_{drv}$$

- For an extraterrestrial observer: pendulum swings back and forth
- For a terrestrial observer: Trajectory of swing changes by $\vec{a}_{cor}$

Micromechanical Gyroscopes

- Example: The Tuning Fork Gyroscope (TFG)

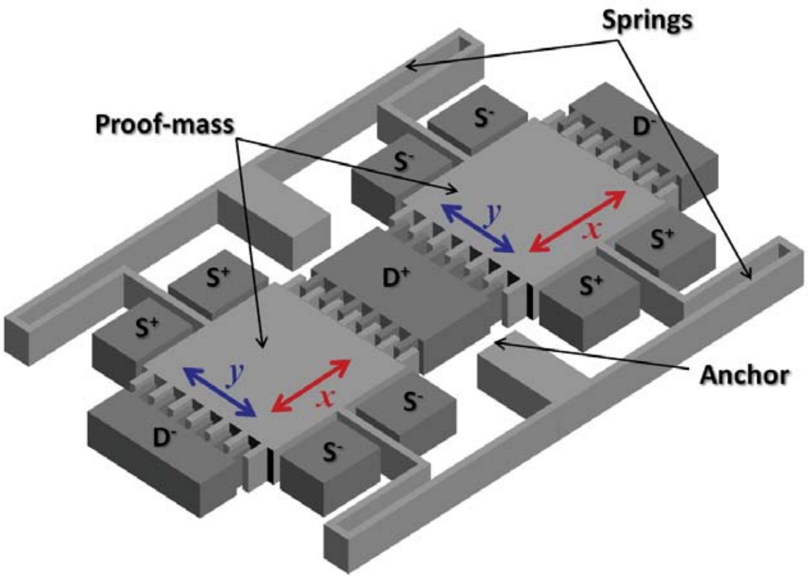

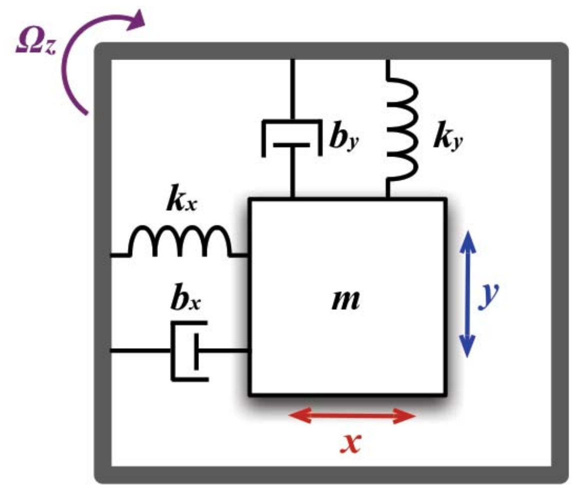

Lumped-Element Model

- Equations of motion of an ideal gyroscope:

Mode 1

$$m\frac{\partial^2 x}{\partial t^2}+b_x\frac{\partial x}{\partial t}+k_x x=F_{elecx}+2m\lambda\Omega_Z\frac{\partial y}{\partial t}$$

Mode 2

$$m\frac{\partial^2 y}{\partial t^2}+b_y\frac{\partial y}{\partial t}+k_y y=F_{elecy}-2m\lambda\Omega_Z\frac{\partial x}{\partial t}$$

Modes of Operation

Rotation-Rate Gyros

- Output proportional to Ω

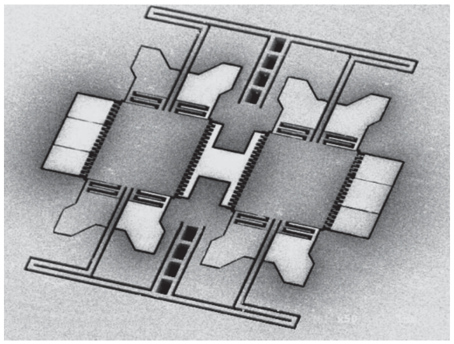

- Mode 1 driven into oscillation
- Mode 2 used to detect rotation

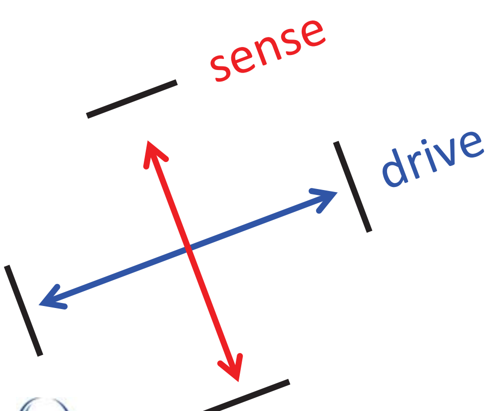

Whole-Angle Mode Gyros

- Output proportional to θ

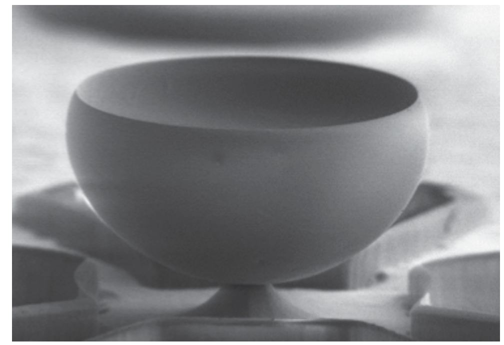

- Free-vibrating structure
- Standing-wave precesses

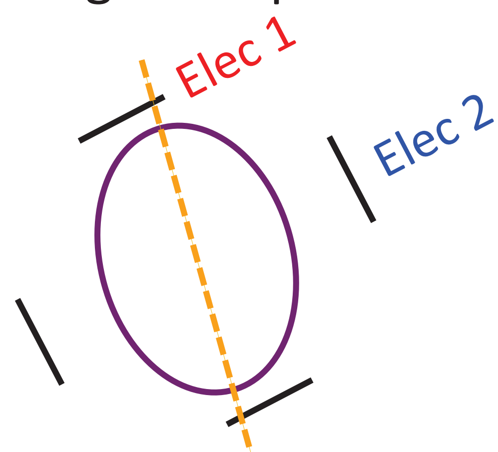

Vibratory Rotation-Rate Gyroscopes

- Two second-order systems
  - Drive (excited into oscillation)
  - Sense (response proportional to rotation-rate Ω)

MODE 1

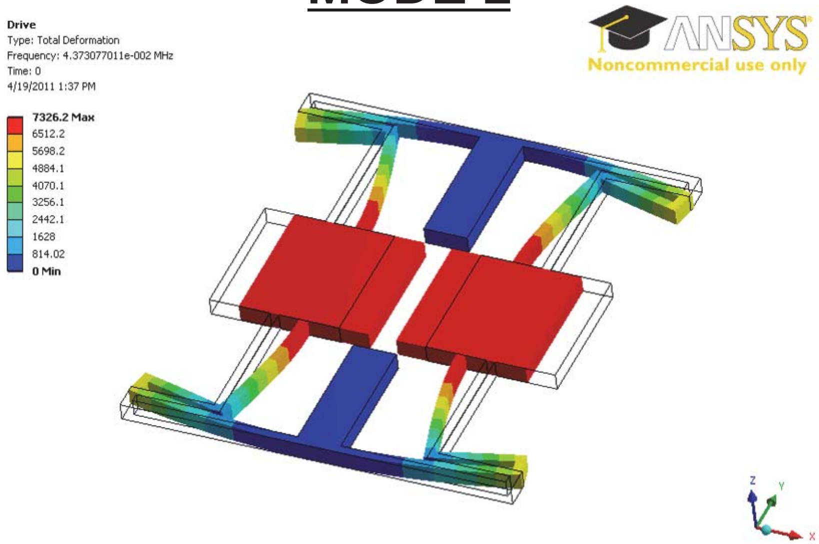

MODE 2

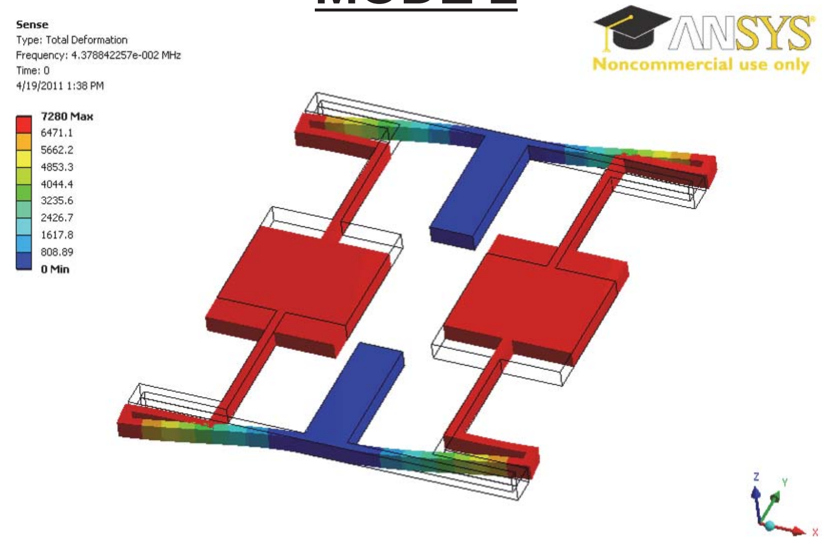

$$m\frac{\partial^2 x}{\partial t^2}+b_x\frac{\partial x}{\partial t}+k_x x=F_{elecx}$$

Coriolis

$$\vec{F}_{cor}=-2m\lambda\,\vec{\Omega}\times\frac{\partial\vec{x}}{\partial t}$$

$$m\frac{\partial^2 y}{\partial t^2}+b_y\frac{\partial y}{\partial t}+k_y y=-2m\lambda\Omega_Z\frac{\partial x}{\partial t}$$

M. F. Zaman et al, JMEMS, 2008

Driving the Gyroscope

- To generate v_{drv}, one mode is driven (usually into oscillation)

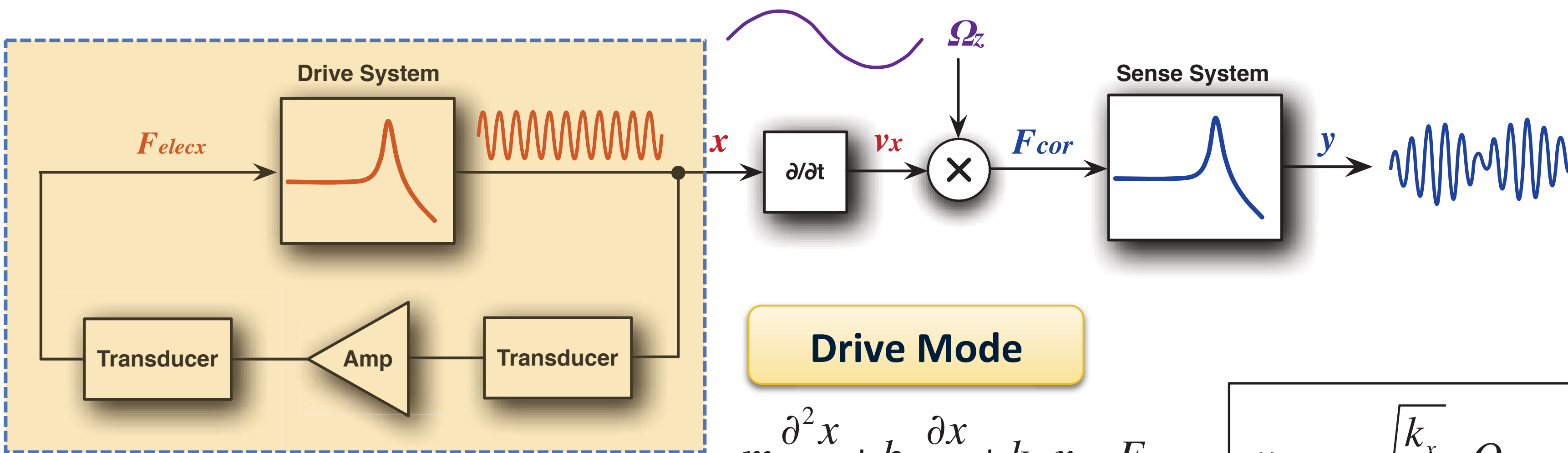

Drive Mode

$$m\frac{\partial^2 x}{\partial t^2} + b_x\frac{\partial x}{\partial t} + k_x x = F_{elecx}$$

$$\omega_{0drv} = \sqrt{\frac{k_x}{m}} \quad Q_{drv} = \frac{\sqrt{k_x m}}{b_x}$$

- Frequency-domain: $\dfrac{X(j\omega)}{F_{elec}(j\omega)} = \dfrac{1}{m}\dfrac{1}{-\omega^2 + \dfrac{\omega_{0drv}}{Q_{drv}} j\omega + \omega_{0drv}^2}$

- At resonance ($\omega = \omega_{0drv}$): $\left|\dfrac{X(j\omega)}{F_{elecx}(j\omega)}\right| = \dfrac{Q_{drv}}{m\omega_{0drv}^2}$ and $\angle\dfrac{X(j\omega)}{F_{elecx}(j\omega)} = -90^{\circ}$

Electrostatic Transducers

Parallel-Plate Transducer

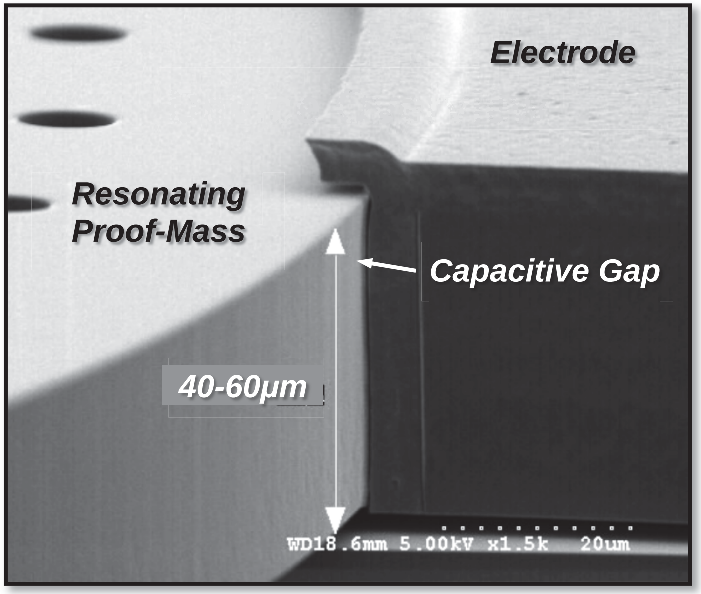

GATech/Qualtré's HARPSS parallel-plate gaps

- ✓ High electromechanical coupling
- ✓ Small and easy to implement
- ✗ Non-linear transfer function

$$\frac{dC}{dx} = \frac{\varepsilon \cdot w \cdot t}{(g_0 - x)^2} \approx \frac{\varepsilon \cdot w \cdot t}{g_0^2}$$

Comb-Drive Actuation

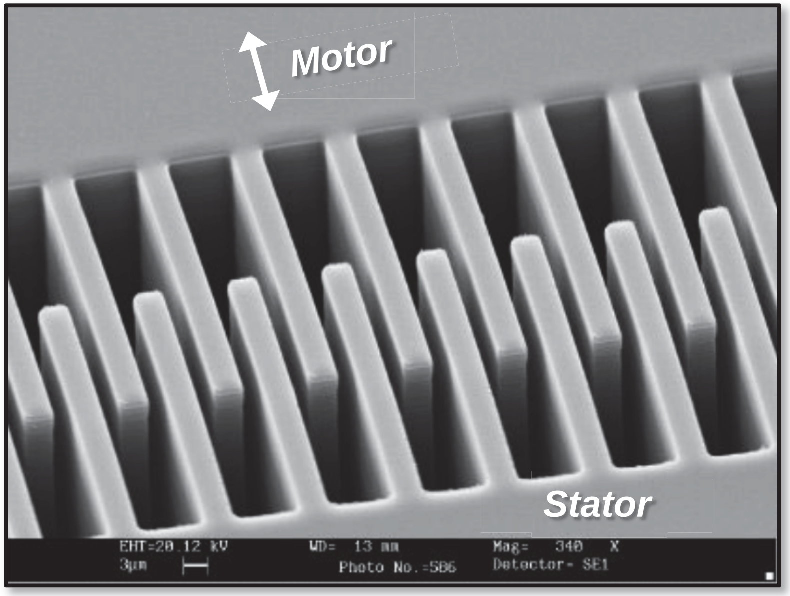

Micralyne DRIE etched comb-drive structures

- ✓ Linear actuation
- ✓ Allows large displacements
- ✗ Low coupling coefficient

$$\frac{dC}{dx} = \frac{\varepsilon \cdot 2n \cdot t}{g_0}$$

Detecting Rotation Rate

- With v_{drv} established, the sense mode responds in presence of Ω

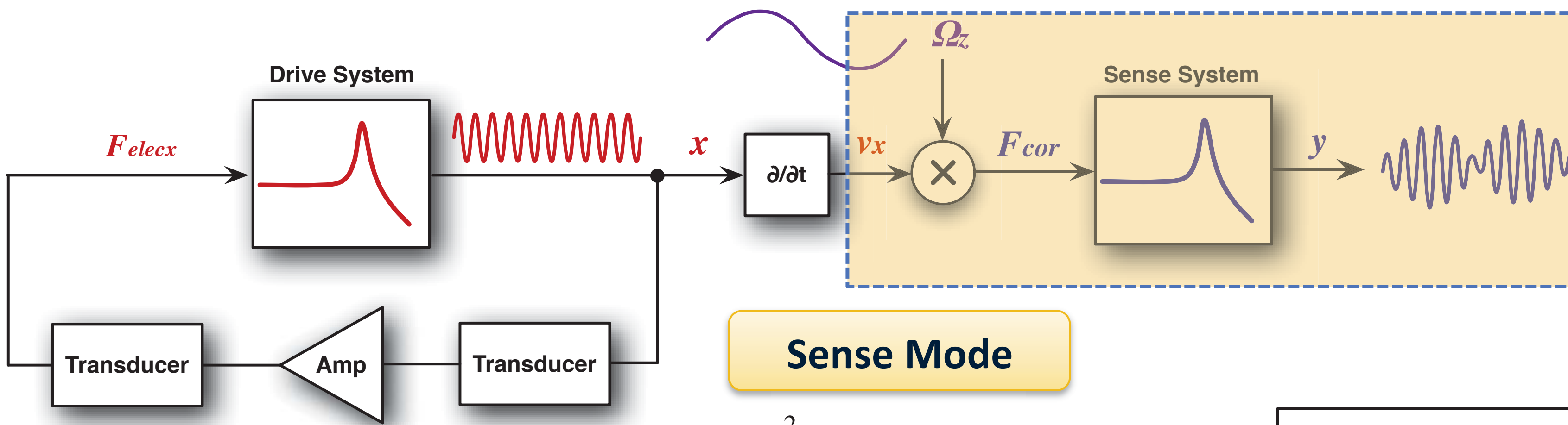

Sense Mode

$$m\frac{\partial^2 y}{\partial t^2} + b_y\frac{\partial y}{\partial t} + k_y y = F_{cor}$$

$$F_{cor} = 2m\lambda\Omega_Z\frac{\partial x}{\partial t}$$

- Frequency-domain: $$\left.\frac{Y(j\omega)}{X(j\omega)}\right|_{\omega=\omega_{0drv}} = 2\lambda\Omega\frac{j\omega_{0drv}}{-\omega_{0drv}^2 + \frac{\omega_{0sns}}{Q_{sns}}j\omega_{0drv} + \omega_{0sns}^2}$$

- But where is ω_{0sns} with respect to ω_{0drv}?

Rate Gyros - Modes of Operation

- Mode-Split: Drive and sense frequencies are different
- Mode-Matched: Drive and sense frequencies are identical

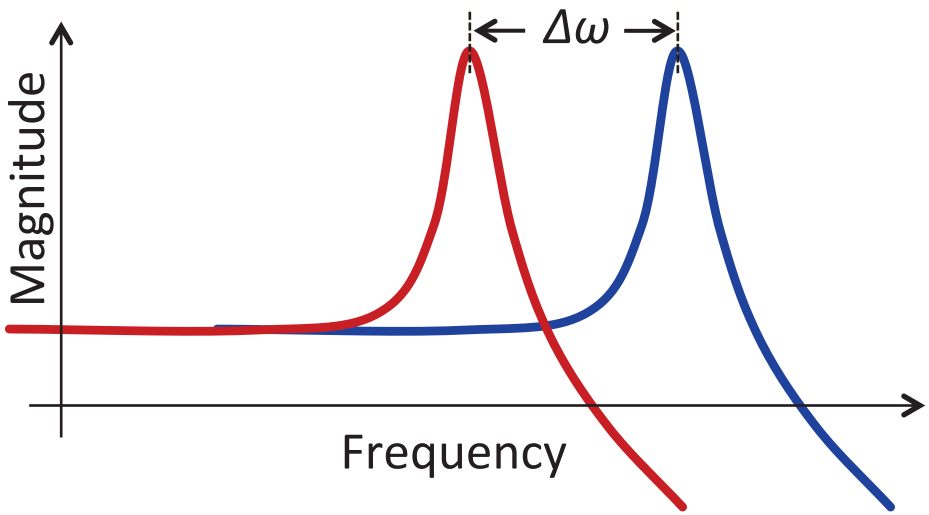

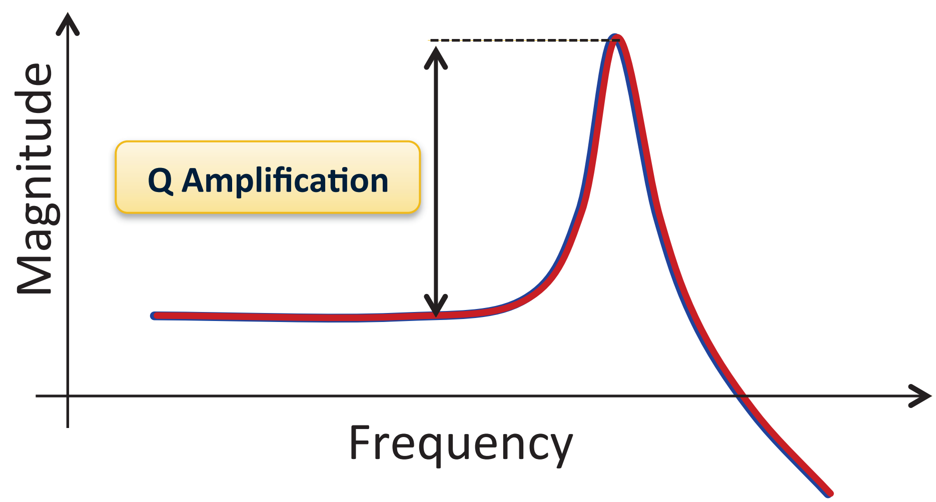

If $\omega_{0drv} << \omega_{0sns}$:

$$\left|\frac{y}{x}\right|_{split} \approx 2\lambda\Omega_Z \frac{\omega_{0drv}}{\omega_{0sns}^2}$$

If $\omega_{0drv} = \omega_{0sns}$:

$$\left|\frac{y}{x}\right|_{matched} = 2\lambda\Omega_Z \frac{Q}{\omega_0}$$

Mode-Split vs. Mode-Matched Gyros

Mode-Split Gyros

- Typically of Tuning-Fork kind

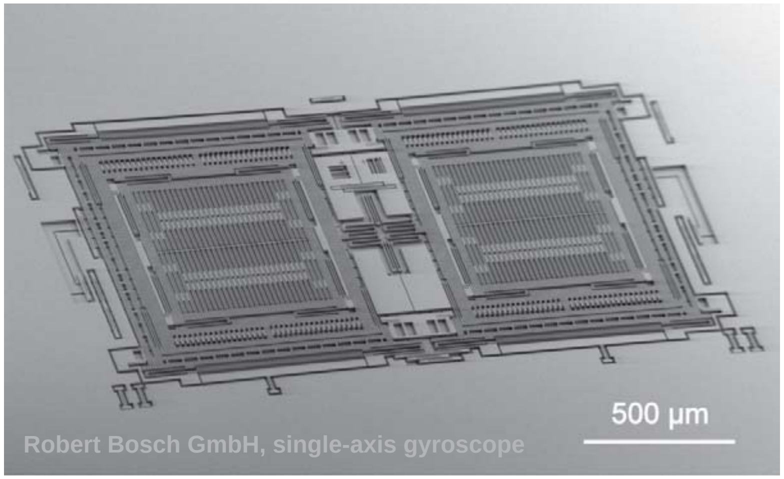

J. Marek, IEEE, ISSCC 2010

- Modes from different mechanisms
- Large BW (accelerometer response)
- Scale factor $\propto 1/\omega^2_{sns}$
  - Large mass (bigger size)
  - Low spring constant (poor reliability)

Mode-Matched Gyros

- Typically axisymmetric

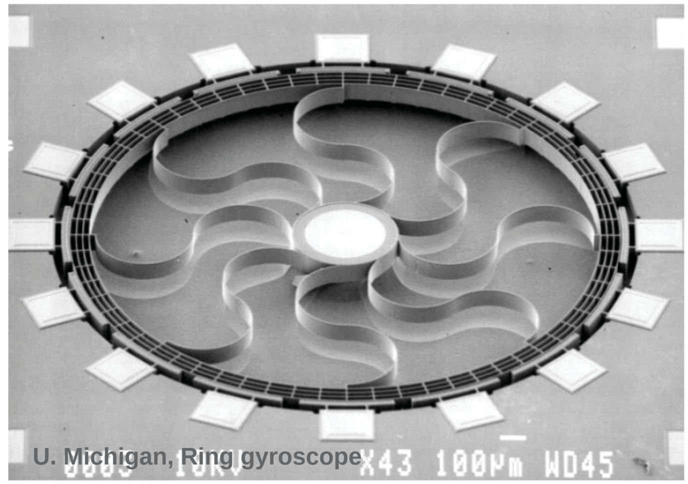

- Inherent degenerate modes
- BW proportional to f_0/Q
- Scale factor $\propto$ Q
  - 10,000 to 1’000,000 larger!!

Mode-Split Rate Gyroscopes

- Typically TFGs → Low resonance frequency (1 – 30 kHz)

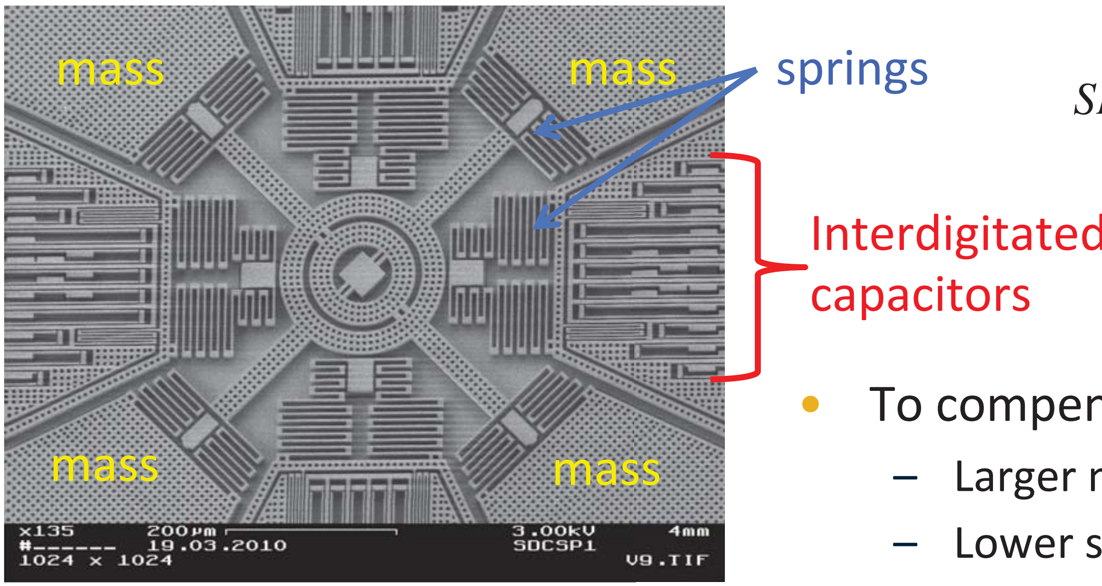

SensorDynamics, 3-axis gyroscope
Source: http://www.i-micronews.com/news/Generation-MEMS-gyroscopes-inertial-combo-sensors-SensorDyn,6375.html

$$SF \propto \frac{x_{drv}\,\omega_{0drv}}{\sqrt{\left(\omega_{0sns}^2 - \omega_{0drv}^2\right)^2 + \frac{\omega_{0sns}^2\,\omega_{0drv}^2}{Q_{sns}}}} \frac{dC}{dx} V_P$$

- To compensate for loss of Q-amplification:
  - Larger mass
  - Lower stiffness
  - Interdigitated and comb capacitors

- For large x_{drv}, high-Q still needed on drive
- In kHz range, high-vacuum required for high Q → <u>GETTERS</u>

Bulk-Acoustic Wave (BAW) Gyroscopes

- Axisymmetric structure → Inherently mode-matched
- Q = 50,000 to 200,000 in 1 to 10 Torr → High sensitivity, low noise
- High f_0 (MHz range)→ Large BW, dynamic range, shock resistance

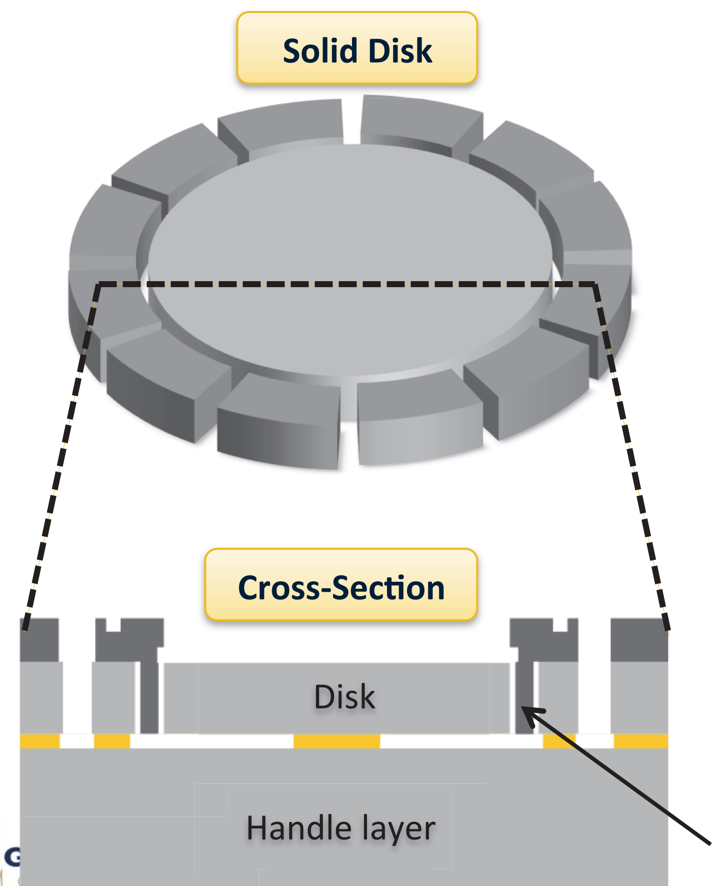

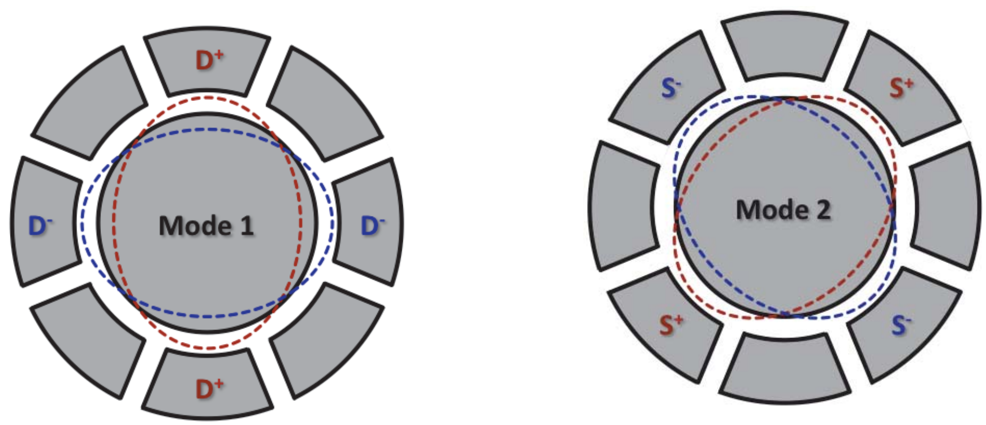

H. Johari et al, MEMS, 2007

- Capacitive nano-gaps
  - Large electromechanical coupling

Operation BAW Rate Gyroscopes

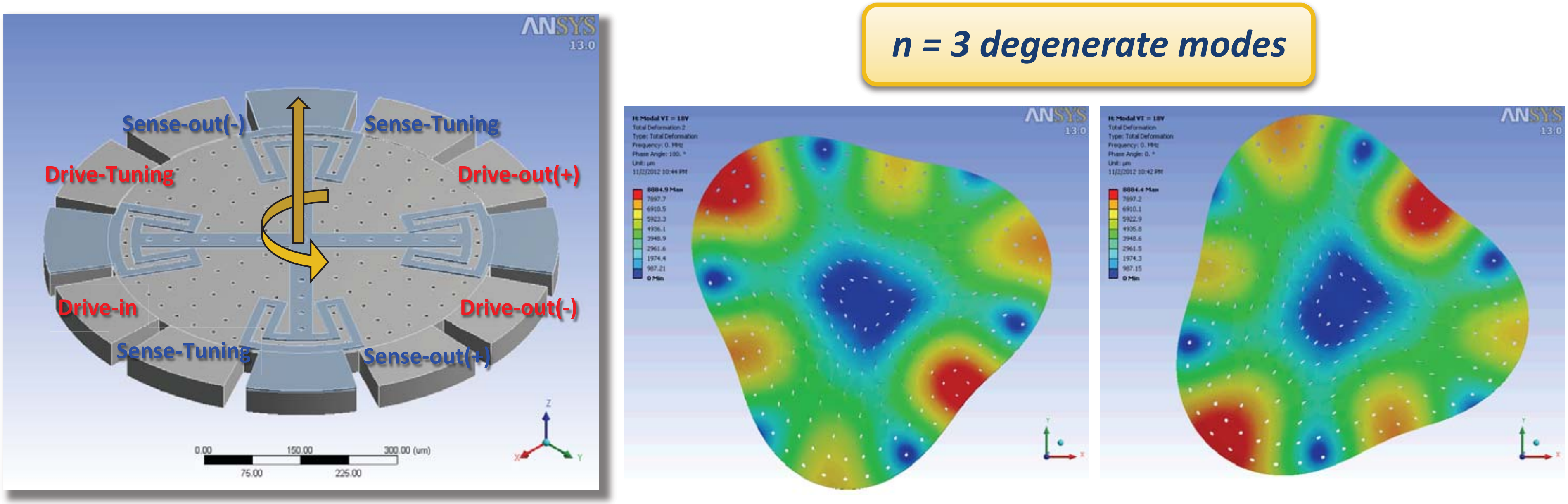

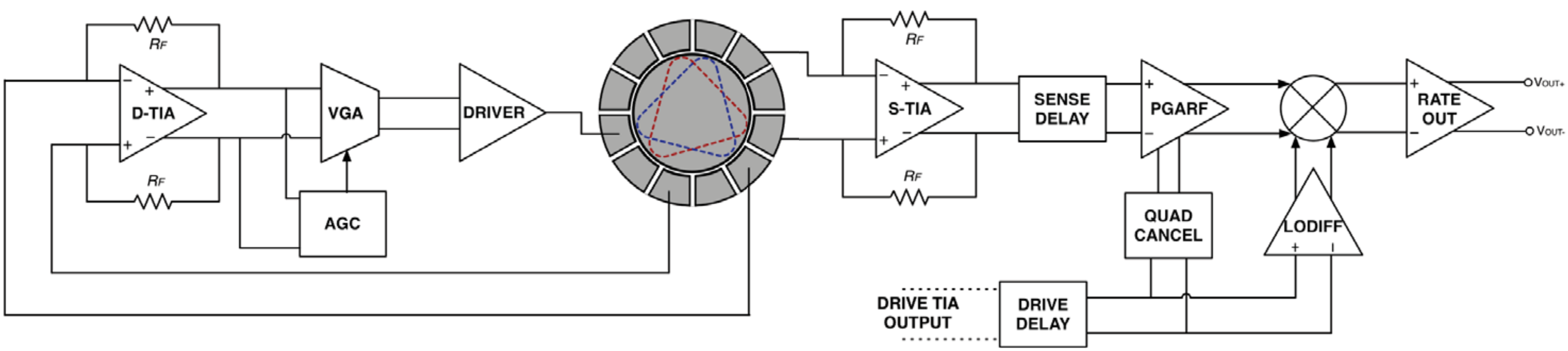

Implementation of BAW Gyroscopes

9.6 MHz BAW Disk Gyro

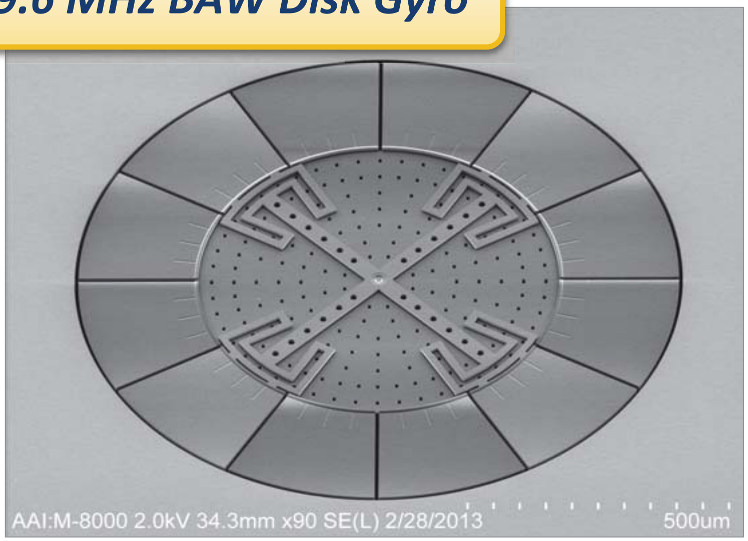

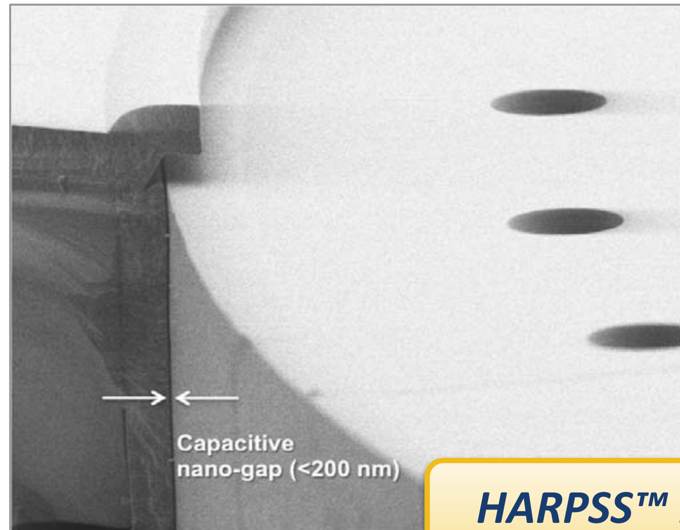

HARPSS™ Process

Wafer-level Package

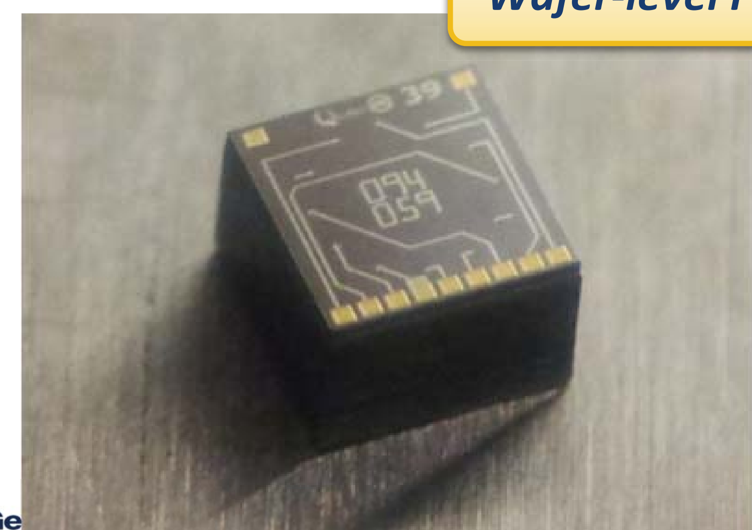

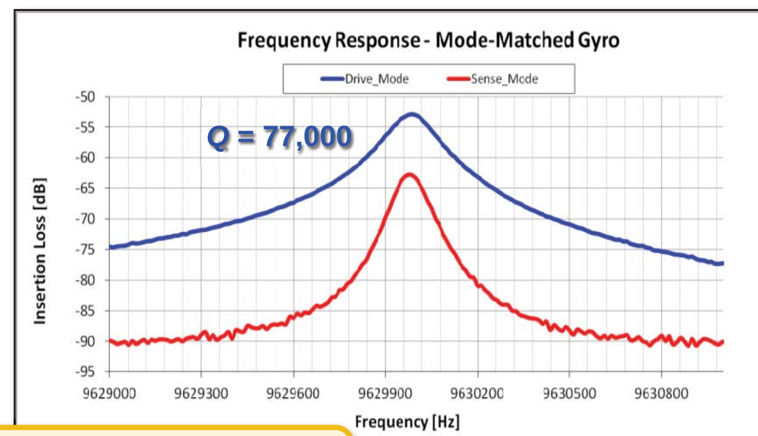

High Q at 1 – 10 Torr

Performance of Capacitive BAW Gyros

Motional Impedance

$$R_m = \frac{2\pi \cdot M_{eff} \cdot g_0^4 \cdot f_{res}}{\left(\varepsilon_0 \cdot A_{elec} \cdot V_P\right)^2 \cdot Q} \quad [\Omega]$$

- Lower is better!
  - High Q (~50,000 @ 1 – 10 Torr)
  - Ultra-small capacitive nano-gaps

Scale Factor

$$SF = \frac{2\pi \cdot \lambda \cdot \varepsilon_0 \cdot A_{elec} \cdot V_P \cdot Q}{180 \cdot \alpha \cdot g_0} \quad [\text{A/(°/s)}]$$

- Higher is better!
  - Independent of frequency!!

Mechanical Noise

$$MNE\Omega = \frac{180 \cdot \alpha}{\pi \cdot \lambda \cdot g_0} \sqrt{\frac{k_B \cdot T}{\pi \cdot M_{eff} \cdot f_{res} \cdot Q}} \quad [(°/s)\sqrt{\text{Hz}}]$$

- Lower is better!
  - High f_{res} & high Q compensate for smaller displacements

Bandwidth

$$BW = \frac{f_{res}}{2Q} \quad [\text{Hz}]$$

- Higher is better!
  - High f_{res} compensates for high Q

Pitch and Roll Annulus Gyroscopes

- High frequency operation (0.5 ~ 1.5 MHz)
- Process compatible with HARPSS™ → air nano-gaps

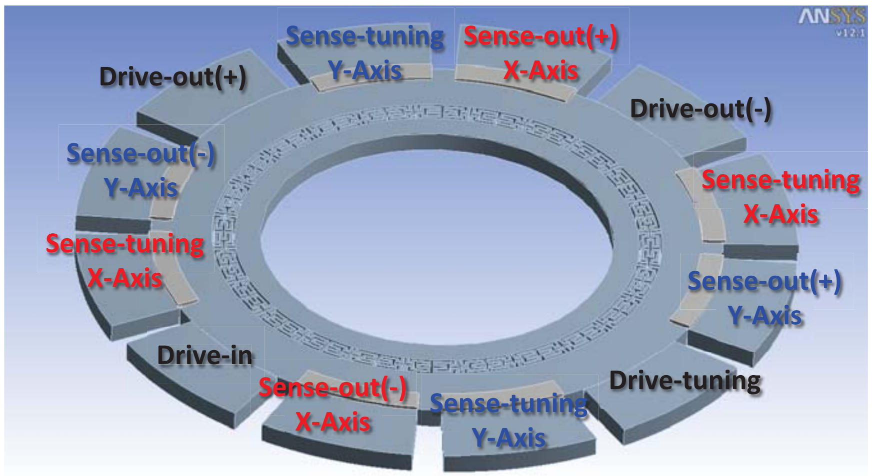

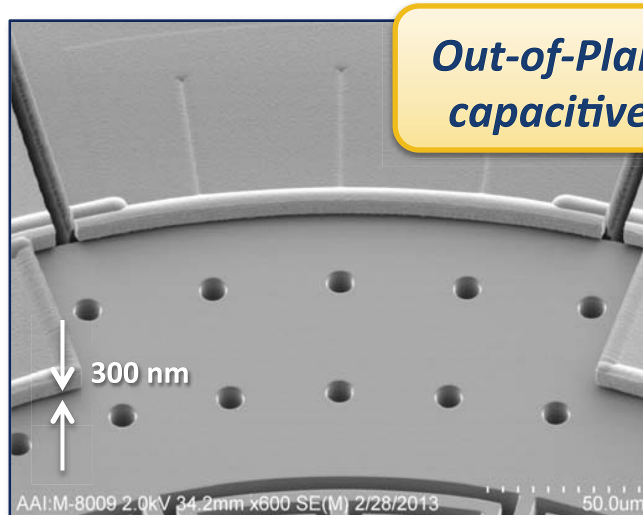

Out-of-Plane HARPSS™ capacitive nano-gaps

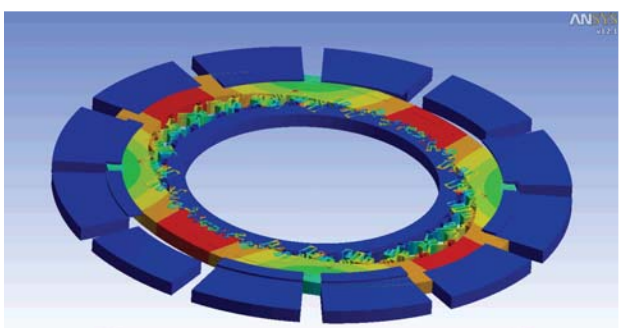

In-plane drive mode

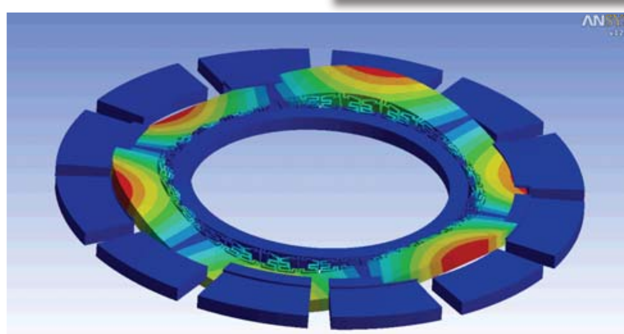

Out-of-plane x-axis sense mode

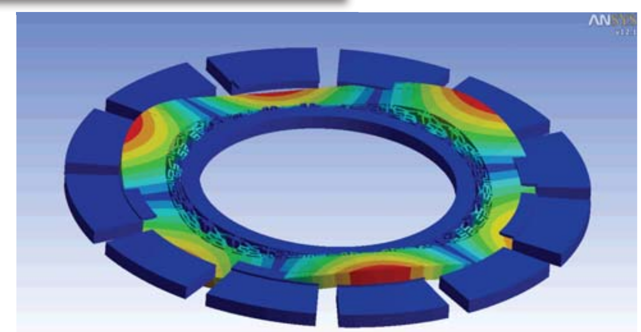

Out-of-plane y-axis sense mode

W. K. Sung et al, TRANSDUCERS, 2011

Annulus Gyroscopes - Response

- Small frequency split (further compensated with electronics)

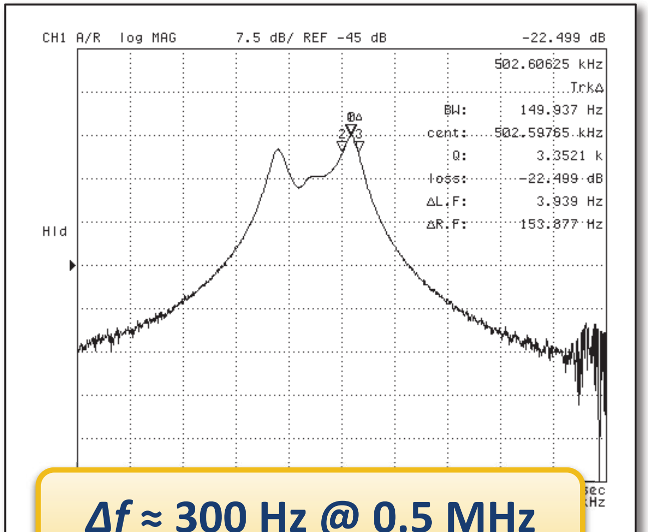

Δf ≈ 300 Hz @ 0.5 MHz

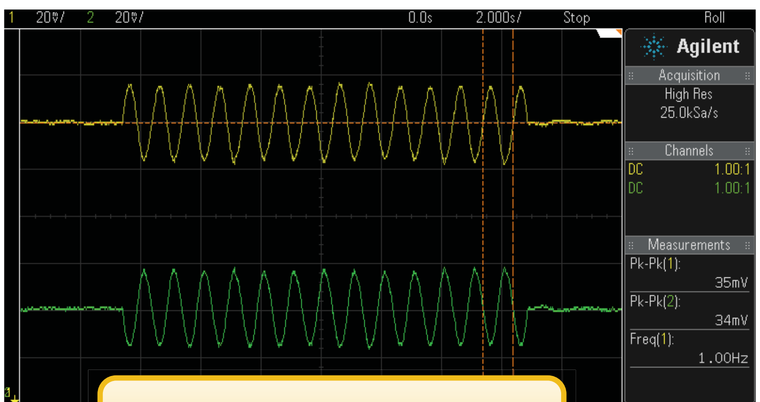

Rate Response

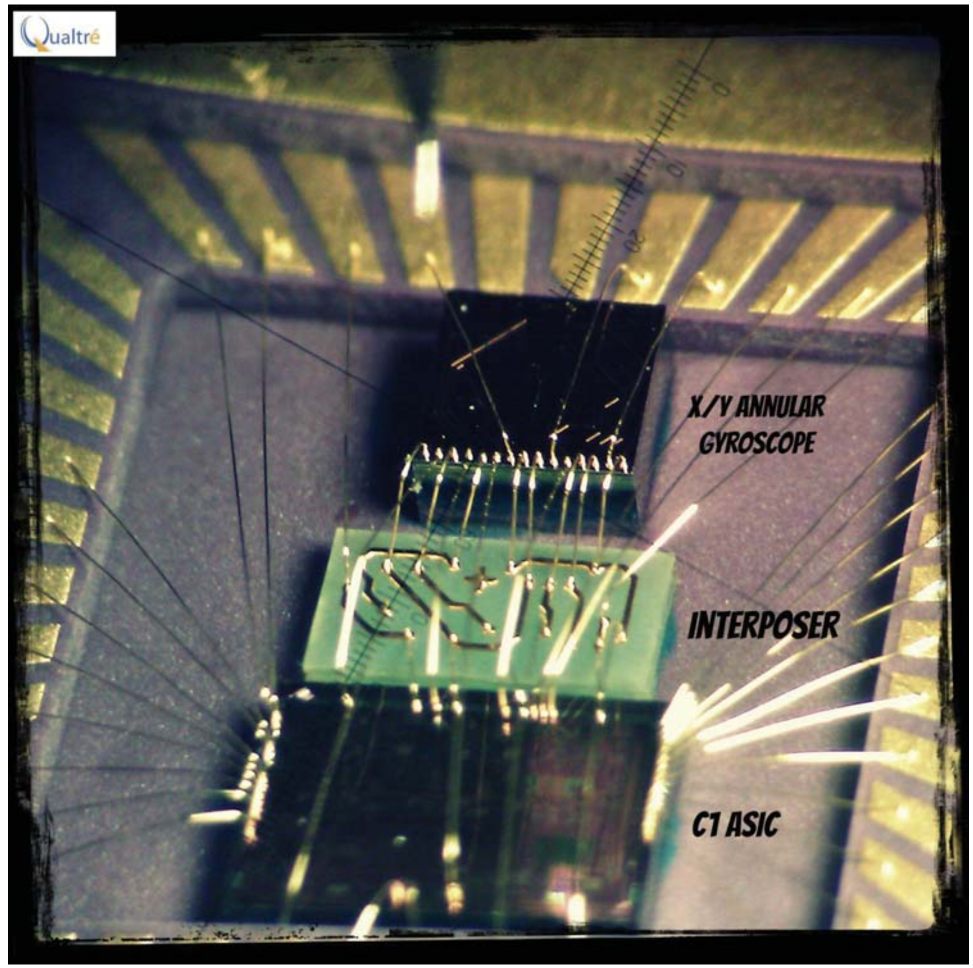

Multi-Degree-of-Freedom Integration

Monolithic TIMU Die

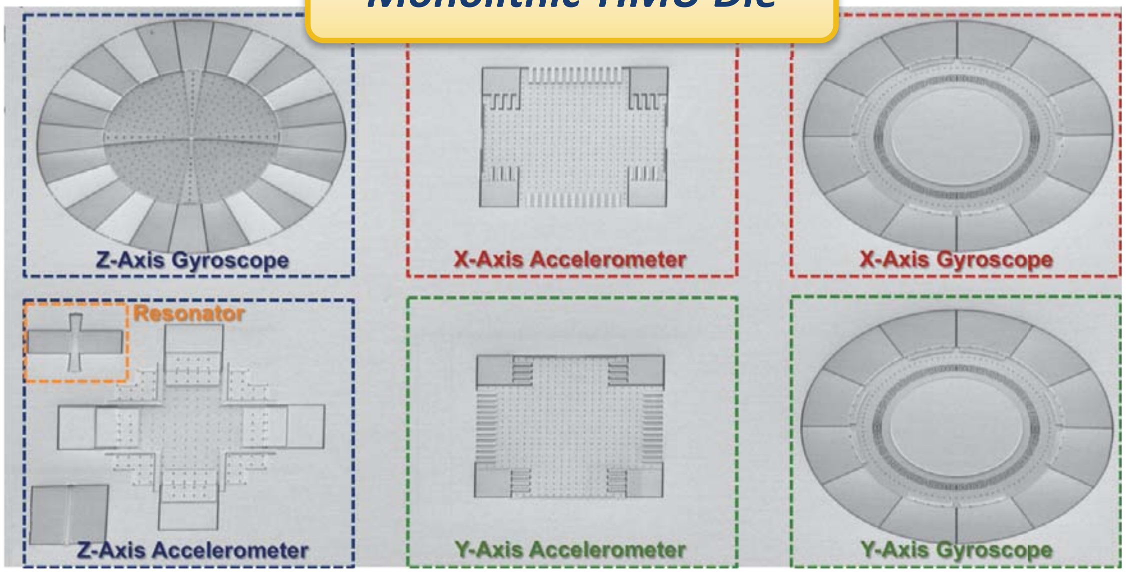

WLP TIMU die

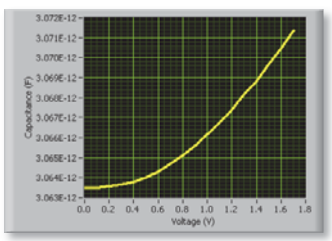

X-Axis Axl. Response

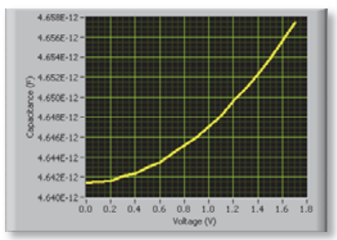

Z-Axis Axl. Response

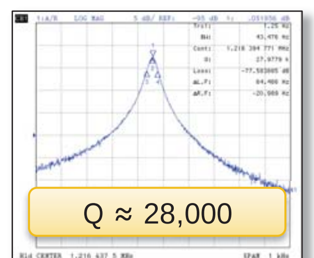

X-Axis Gyro Response

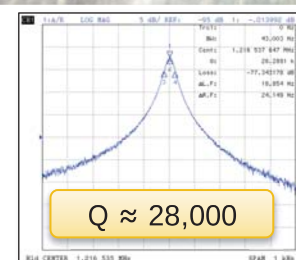

Y-Axis Gyro Response

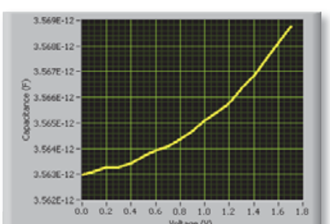

Y-Axis Axl. Response

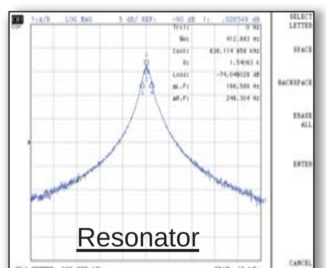

Resonator

Z-Axis Gyro Response

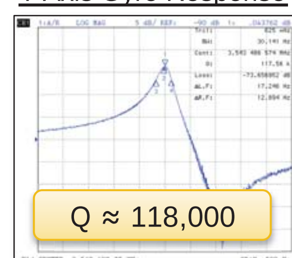

Error Sources in Mode-Matched Gyros

- Mode 1:

$$m_{11}\ddot{q}_1(t)+d_{11}\dot{q}_1(t)+k_{11}q_1(t)=-2\lambda m_{22}\dot{q}_2(t)\Omega(t)$$

Coriolis coupling

- Mode 2:

$$m_{22}\ddot{q}_2(t)+d_{22}\dot{q}_2(t)+k_{22}q_2(t)=2\lambda m_{11}\dot{q}_1(t)\Omega(t)$$

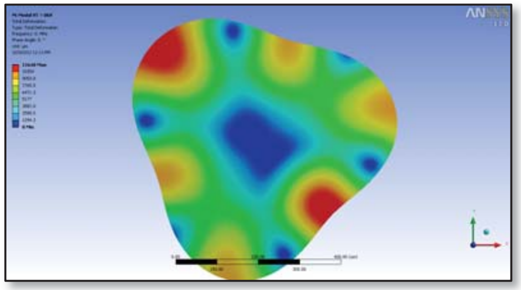

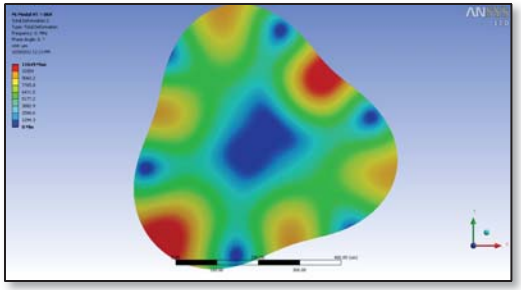

- Ideal gyroscope: $\omega_{0_1}=\sqrt{\frac{k_{11}}{m_{11}}}=\omega_{02}=\sqrt{\frac{k_{22}}{m_{22}}}$ → $\Delta\omega_0=0$

- Anisoelasticity: $k_{22}\neq k_{11}$
- Anisoinertia: $m_{22}\neq m_{11}$

$\omega_{0_1}\neq\omega_{02}$

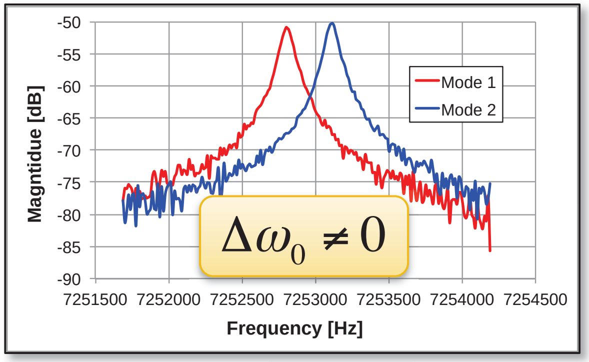

Compensating for Frequency-Split

- Electrostatic Spring Softening

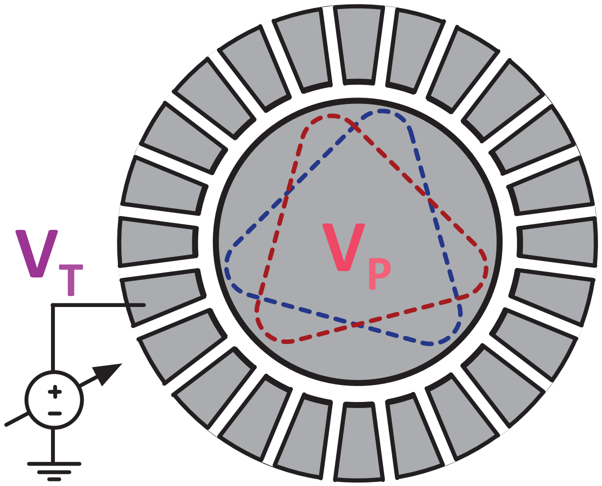

Aligned with mode 1

$$\omega_{01} = \sqrt{\frac{k_{11mech} - k_{11elec}}{m_{11}}}$$

$$k_{11elec} = \frac{\varepsilon A}{g_0^3} \sum_{j=1}^{l} \left(V_P - V_{T,j}\right)^2$$

Spring softening

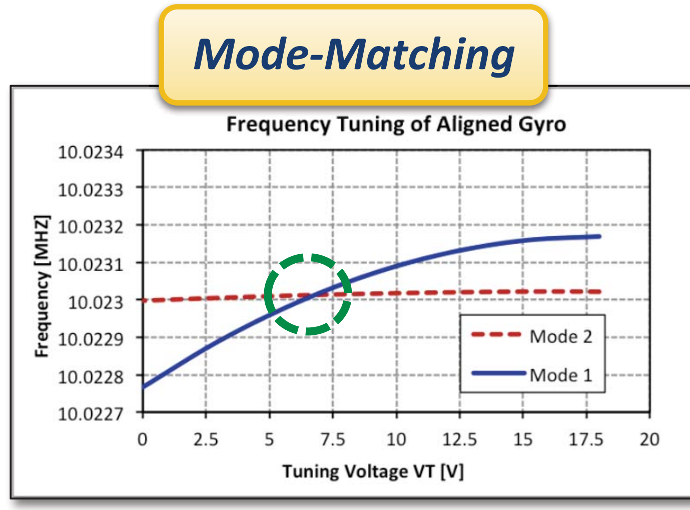

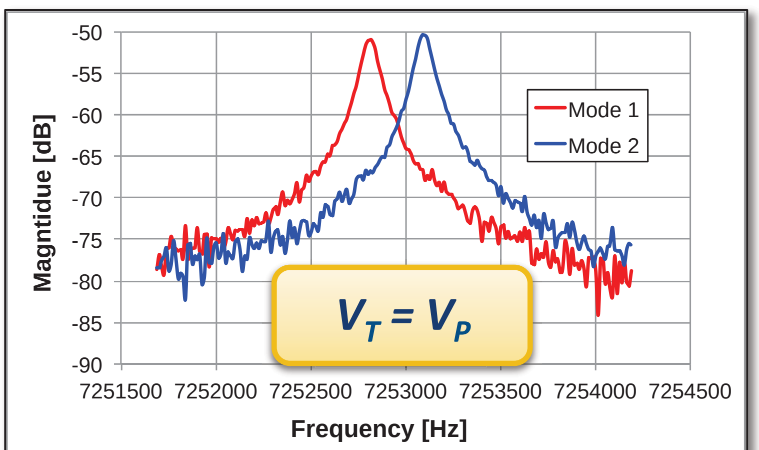

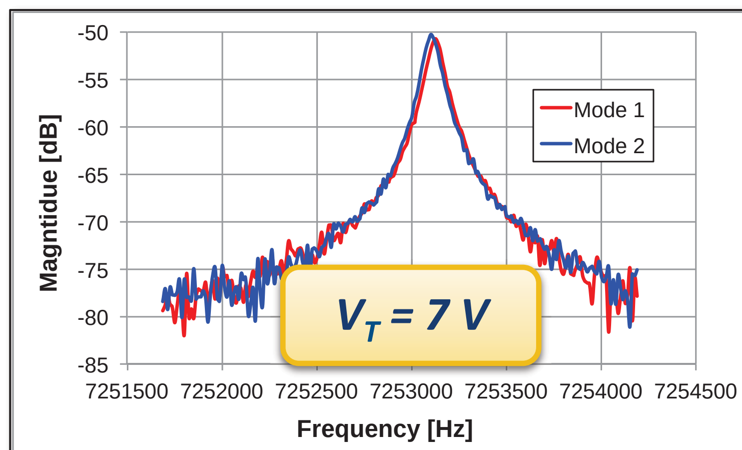

Mode-to-Mode Coupling

- Ideal gyroscope with uncoupled modes

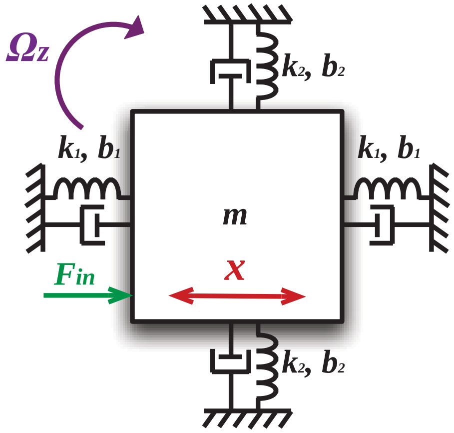

Coriolis Effect

$$F_{cor} = 2m\lambda\Omega_Z \frac{\partial x}{\partial t}$$

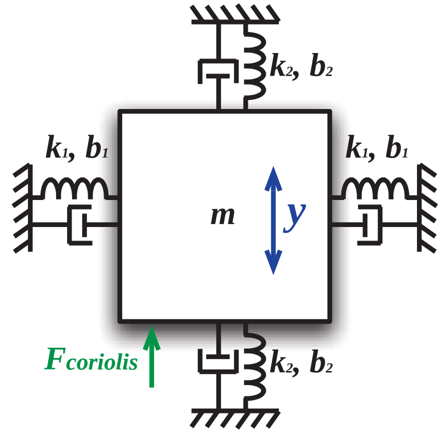

- Imperfect gyroscope with <u>coupled</u> modes

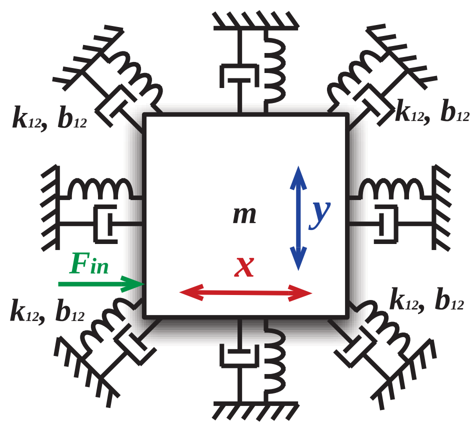

$$m\ddot{q}_1(t) + d_{11}\dot{q}_1(t) + d_{12}\dot{q}_2(t) + k_{11}q_1(t) + k_{12}q_2(t) = -2\lambda m\dot{q}_2(t)\Omega(t)$$

Damping coupling — Stiffness coupling — Coriolis coupling

$$m\ddot{q}_2(t) + d_{22}\dot{q}_2(t) + d_{21}\dot{q}_1(t) + k_{22}q_2(t) + k_{21}q_1(t) = 2\lambda m\dot{q}_1(t)\Omega(t)$$

Stiffness Coupling

- Mode 1 displacement generates force that couples to Mode 2

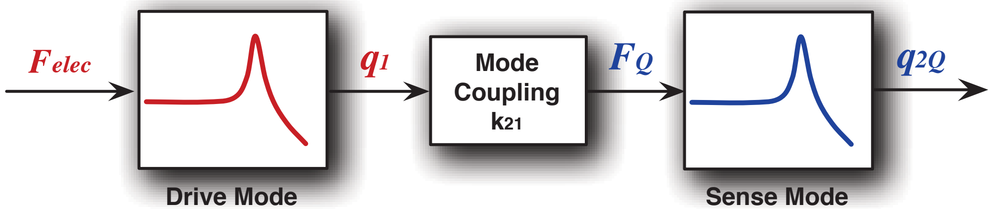

If $k_{11} = k_{22}$ (i.e. $\Delta\omega$ close to 0):

$$\angle \frac{q_{2Q}}{q_1} \approx -90^{\circ}$$

Quadrature

- Electrostatic mode-decoupling:

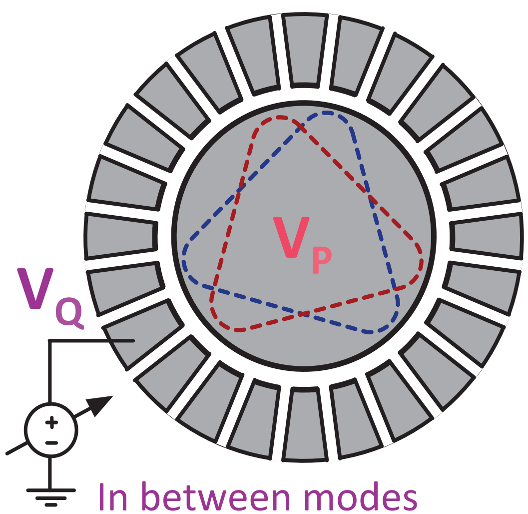

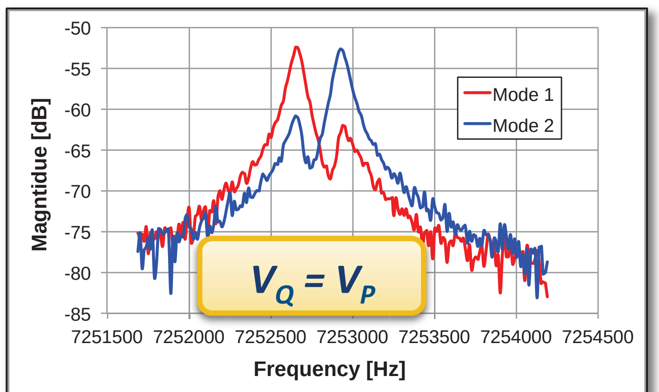

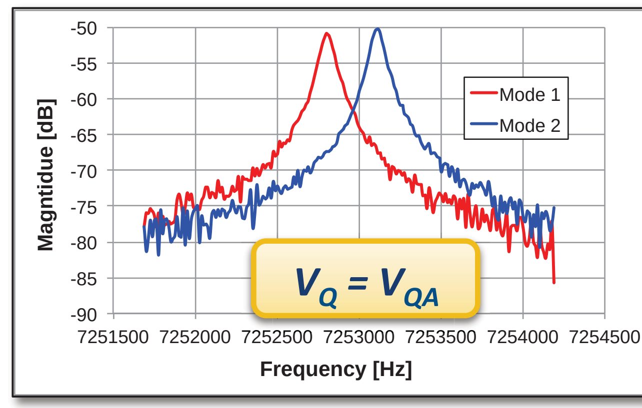

- @ $V_Q = V_{QA}$ → $q_{2Q} = 0$ (modes decoupled)

Damping Coupling

- Mode 1 velocity generates force that couples to Mode 2

$$\ddot{q}_{2I}(t)+\frac{\omega_{0_2}}{Q_2}\dot{q}_{2I}(t)+\frac{b_{21}}{m}\dot{q}_1(t)+\omega_{0_2}^2\,q_{2I}(t)=0$$

- For a mode-matched gyroscope:

$$\left.\frac{q_{2I}(\omega)}{q_1(\omega)}\right|_{\omega=\omega_{0_1}=\omega_{02}}=-\frac{b_{21}Q_2}{m\omega_{0_1}}\angle 0^0$$

- Comparing with Coriolis coupling due to rotation rate

$$\ddot{q}_{2c}(t)+\frac{\omega_{0_2}}{Q_2}\dot{q}_{2c}(t)+\omega_{0_2}^2\,q_{2c}(t)=2\lambda\Omega(t)\dot{q}_1(t)$$

- For a mode-matched gyroscope:

$$\left.\frac{q_{2c}(\omega)}{q_1(\omega)}\right|_{\omega=\omega_{0_1}=\omega_{02}}=\frac{2\lambda Q_2}{\omega_{0_1}}\Omega(\omega')\angle 0^0$$

q_{2I} is indistinguishable from q_{2c}

Loss Mechanisms in Resonant Gyros

- Q in resonant gyroscopes is a combination of different effects:

$$\frac{1}{Q}=\frac{1}{Q_{\mathrm{SFD}}}+\frac{1}{Q_{\mathrm{TED}}}+\frac{1}{Q_{\mathrm{anchor}}}+\frac{1}{Q_{\mathrm{surface}}}+\frac{1}{Q_{\mathrm{intrinsic}}}$$

Squeeze-Film Damping	***Thermoelastic Damping***	***Anchor Loss***

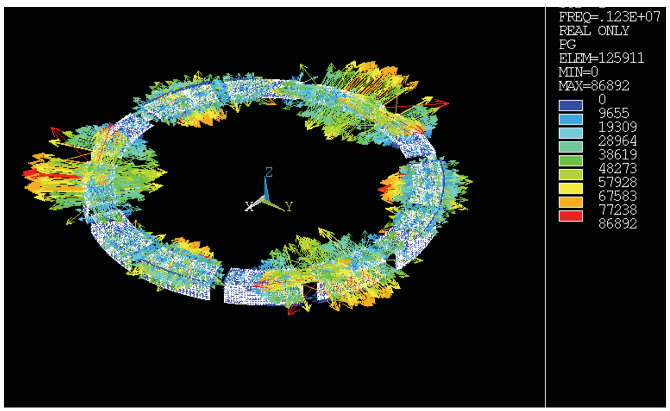

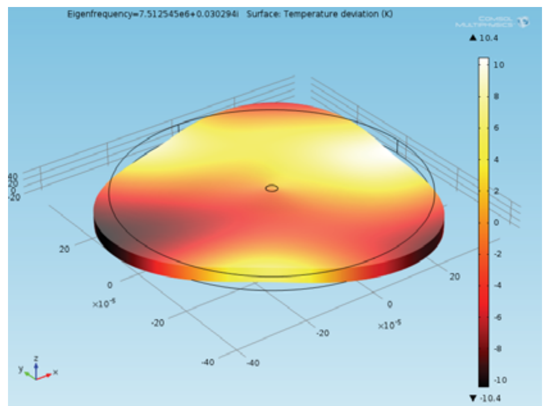

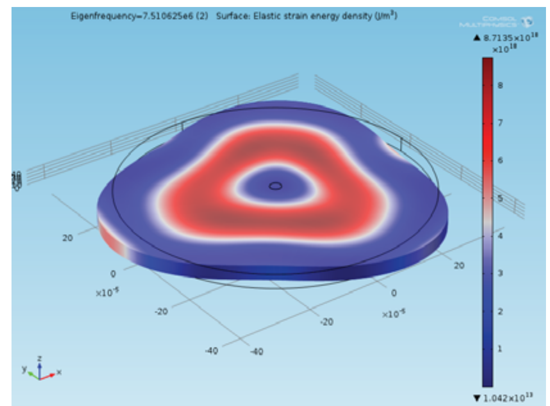

$$\frac{1}{Q_{SFD}} \propto \frac{\mu_{eff}}{g_0^3}\frac{1}{1+\dfrac{j\omega}{\omega_c}}$$

Higher Q at higher freq.

$$\frac{1}{Q_{TED}}=\left(\frac{E\alpha^2 T_0}{C_v}\right)\sum_n \frac{\omega_{mech}\tau_n}{1+\left(\omega_{mech}\tau_n\right)^2} f_n$$

Depends on CTE and therm. modes

$$\frac{1}{Q_{anchor}}=\frac{1}{2\pi}\frac{W_{resonator}}{\Delta W_{anchor}}$$

SED @ anchor

Piezoelectric Square Gyroscope

- Capacitive transducers, well established in sensors, but:
  - Low electromechanical coupling coefficients
  - Non-linear (Parallel plate)
- Piezoelectric transduction → widely used in resonators

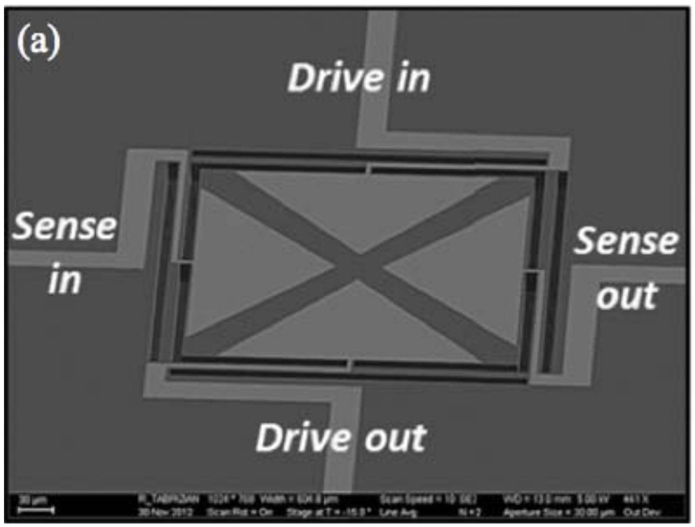

R. Tabrizian, et. al., JMEMS, 2013

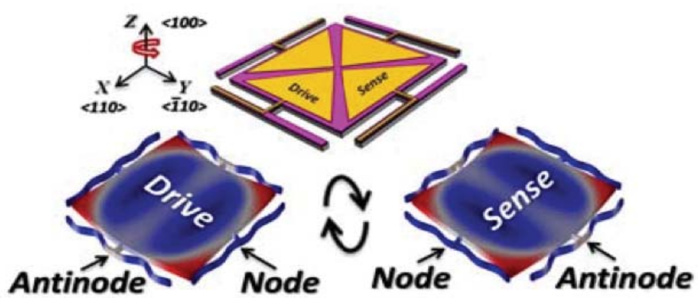

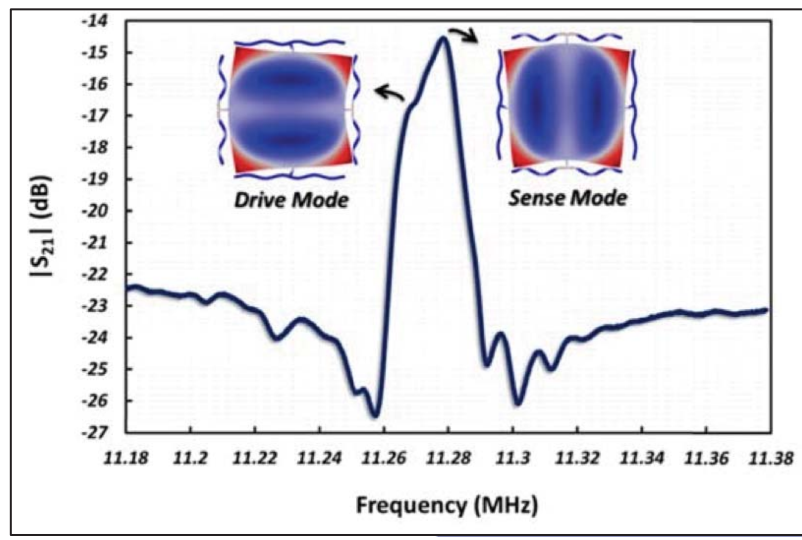

Lamb-Wave Mode Pairs

Whole-Angle Mode Gyroscopes

- Also known as rate-integrating gyroscopes (RIG)
- Strap-down navigation utilizes angle and displacement information

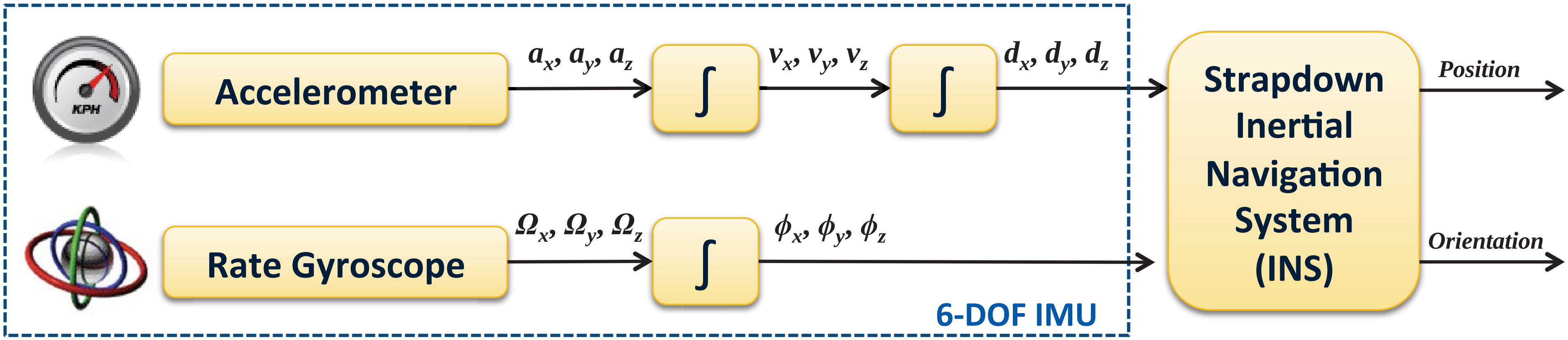

- Integration step introduces error and accumulates drift
- Whole-angle mode → output proportional to angle, not rate

Operation of Whole-Angle Mode Gyros

- Based on relative measurement with respect to a standing-wave
- Similar to the Foucault Pendulum example

Antinode Aligned to Reference

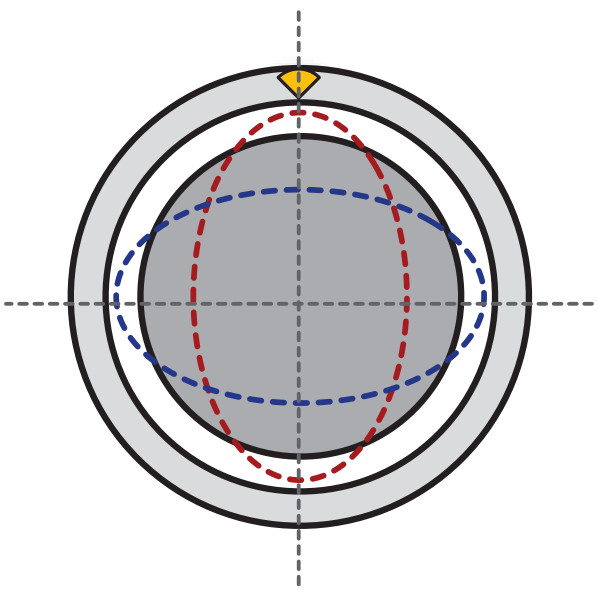

Angular gain

$$\frac{\lambda}{2} = \frac{27}{90} \approx 0.3$$

Structure Rotated 90º

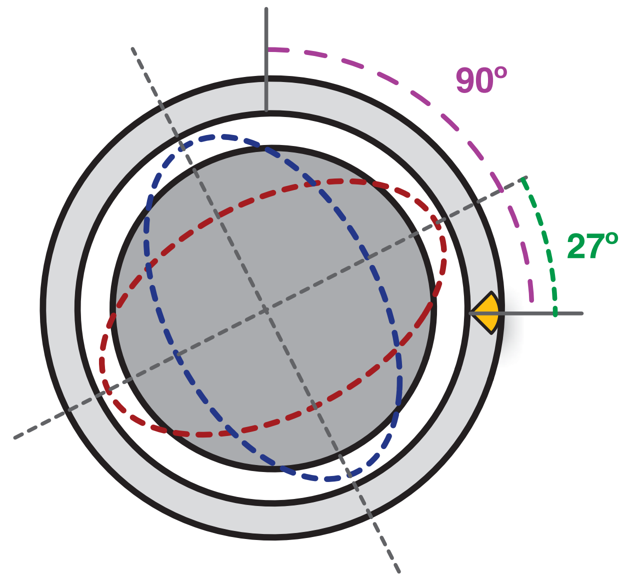

- Anti-nodes precess with respect to reference frame
- The angular gain factor → very stable parameter

But Why Precession?

- First discovered by G.H. Bryan (circa 1890)

Vibrating Wire

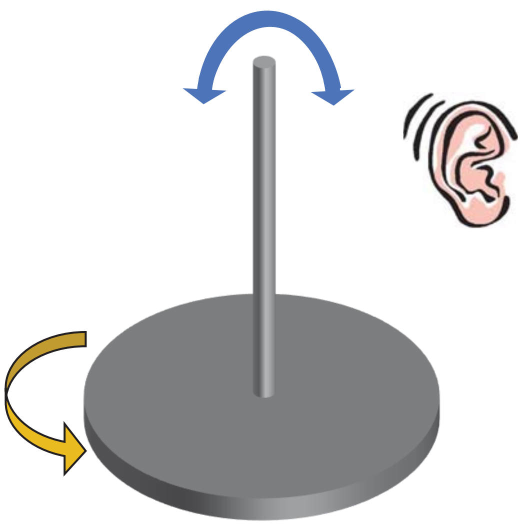

Continuous sound

Tuning Fork

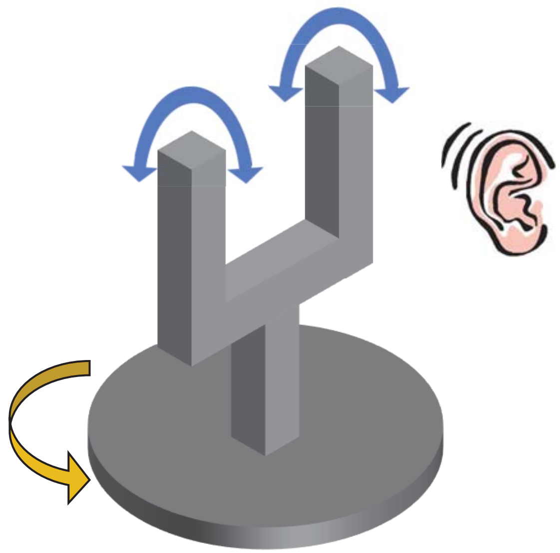

Intermittent sound

Wineglass

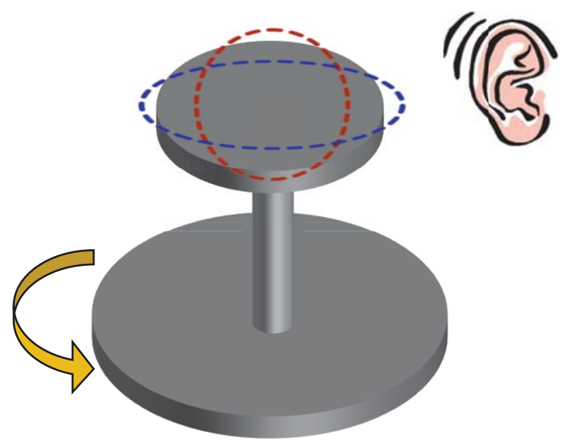

2.4 beats per revolution

- Nodes → no radial component (i.e. no Coriolis effect)
- Antinodes → Maximum radial displacement (i.e. max Coriolis)
- Thus, antinodes have to rotate much faster than nodes

Detection of Rotation Angle

- Breaking down the vibration into orthogonal components:

$$\frac{q_2}{q_1} = \tan 2\theta$$

- θ is the pattern angle → Related to rotation angle through λ

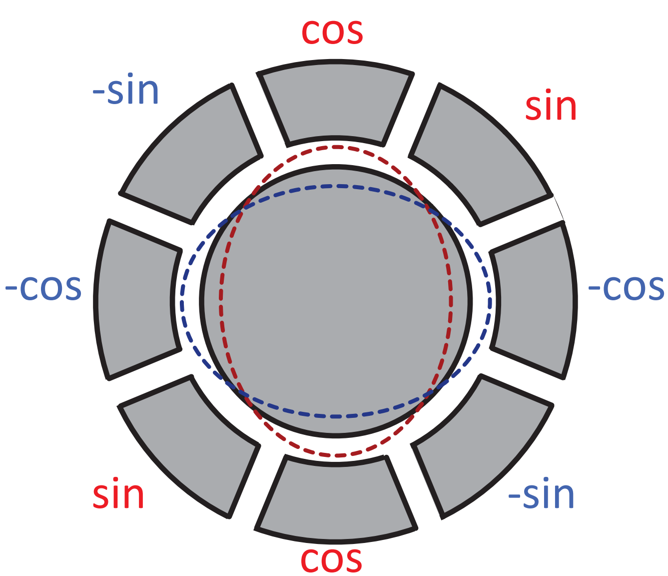

- Two sets of differential electrodes
  - Cosine electrodes: $q_1 * \cos(\omega_0 t)$
  - Sine electrodes $q_2 * \sin(\omega_0 t)$
- q_1 and q_2 obtained by demodulation
- arctan of their ratio → θ

MEMS Whole-Angle Mode Gyros

Example 1

Cylindrical rate-integrating gyroscope (CING)

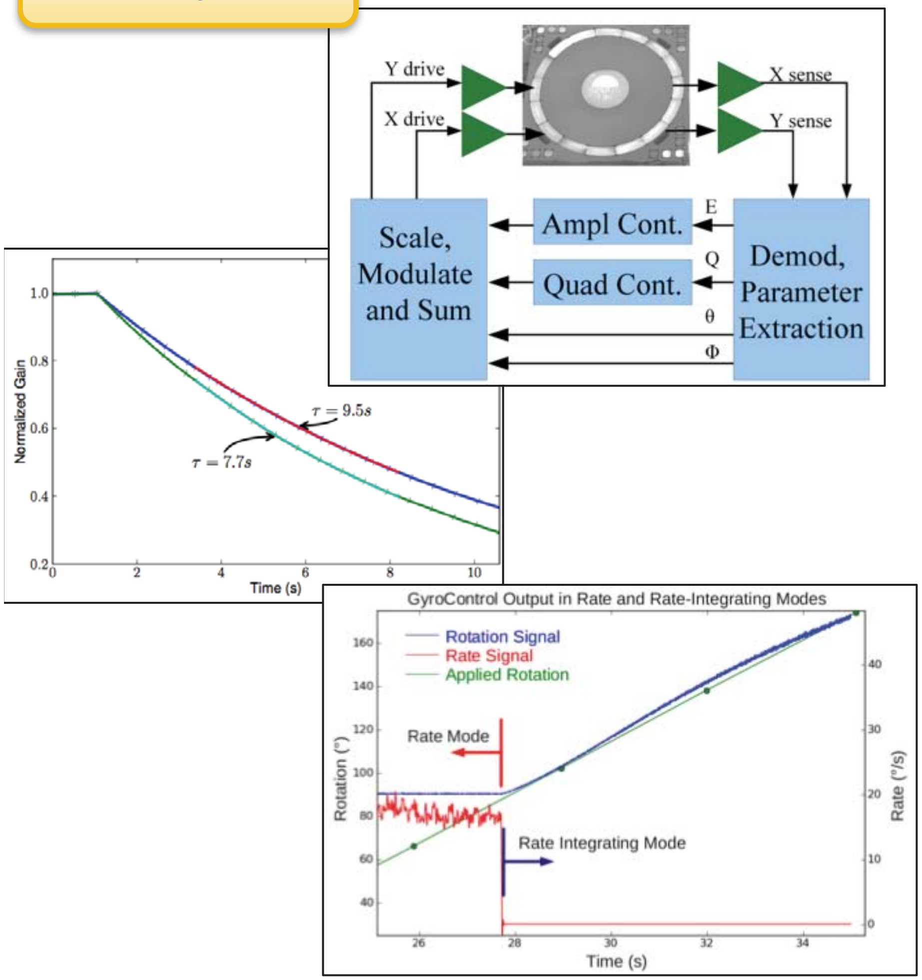

J.A. Gregory, Doctoral Thesis, U. Michigan, 2012

Example 2

Quad-mass tuning fork gyroscope

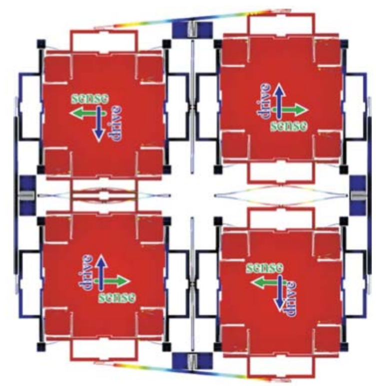

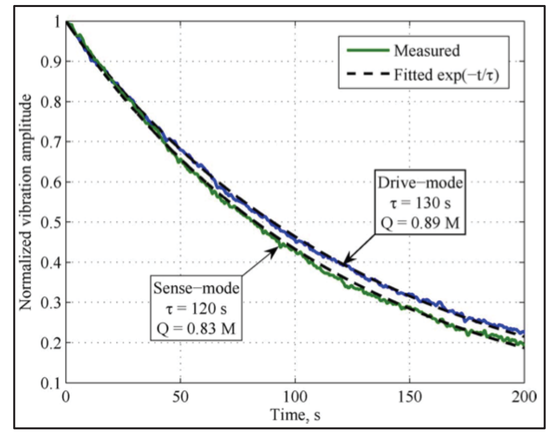

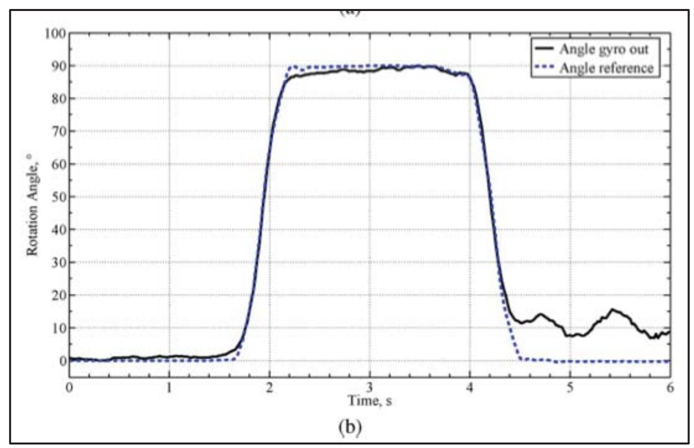

A.A. Trusov, et. Al., IEEE Sensors Journal, 2011

Limitations of MEMS Whole-Angle Gyros

- To operate, pattern of vibration should not be perturbed
- But, amplitude of vibration decays with time → limited Q

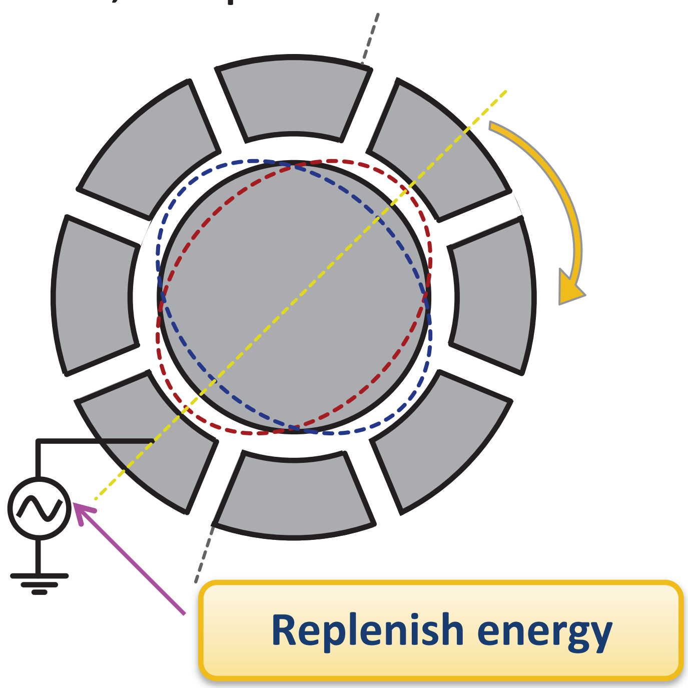

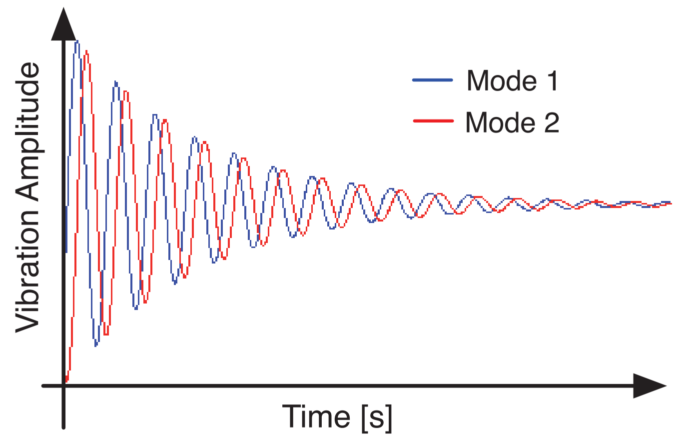

- Long decay times needed
- High Q, low frequency
  - MEMS hemispherical resonator gyros

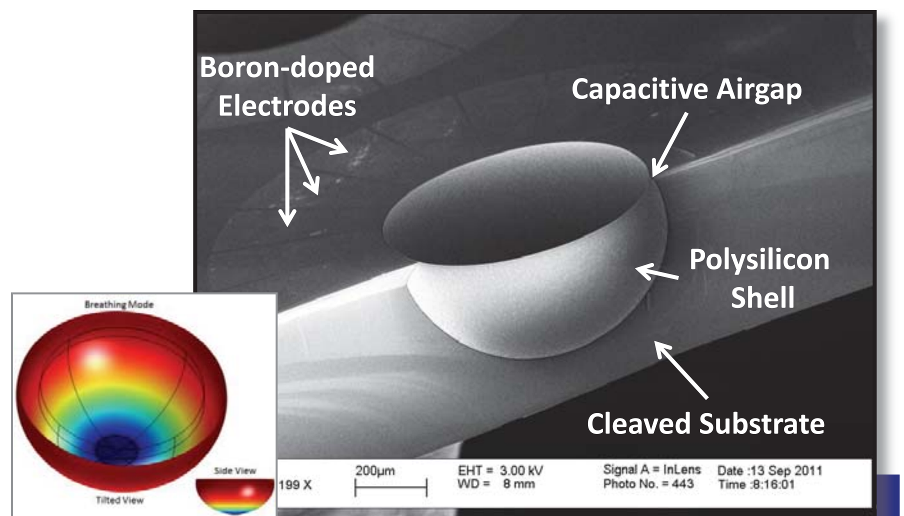

Georgia Institute of Technology
Qualtré

Summary

- Improvements in resolution still required for personal navigation
- Shift in design methodology is imminent to achieve performance
- Vibration and shock immunity are more important than thought
- High-frequency BAW gyros:
  - Rugged structures with clear advantages over TFG designs
  - Easy to integrate into monolithic multi-DOF units
- Whole-angle MEMS gyros → plenty of room for improvement

References

[1] N. Yazdi, F. Ayazi, and K. Najafi, "Micromachined inertial sensors," Proc. IEEE, vol. 86, no. 8, pp. 1640–1659, Aug. 1998.

[2] Bernstein, Jon, et al. "A micromachined comb-drive tuning fork rate gyroscope." *Micro Electro Mechanical Systems, 1993, Proceedings An Investigation of Micro Structures, Sensors, Actuators, Machines and Systems. IEEE.*. IEEE, 1993.

[3] Larsen, Michael, and M. Bulatowicz. "Nuclear Magnetic Resonance Gyroscope: For DARPA's micro-technology for positioning, navigation and timing program." *Frequency Control Symposium (FCS), 2012 IEEE International*. IEEE, 2012.

[4] STMicro L3G3250A Reverse costing, Yole Développement, 2012.

[5] Seeger, Joe, Martin Lim, and Steve Nasiri. "Development of High-Performance, High-Volume Consumer MEMS Gyroscopes." *Technical Digest Solid-State Sensor, Actuator and Microsystems Workshop, Hilton Head Island*. 2010.

[6] M.F. Zaman, A. Sharma, Z. Hao, and F. Ayazi, "A Mode-Matched Silicon-Yaw Tuning-Fork Gyroscope with Subdegree-Per-Hour Allan Deviation Bias Instability," IEEE Journal of Microelectromechanical Systems, Vol. 17, Issue 6, December 2008, pp. 1526-1536.

[7] M.F. Zaman, A. Sharma, and F. Ayazi, "The Resonating Star Gyroscope: A Novel Multiple-Shell Gyroscope with sub-5 deg/hr Allan Deviation Bias Instability," IEEE Sensors Journal, Volume 9, Issue 6, June 2009, pp. 616-624.

[8] F. Ayazi and K. Najafi, "A HARPSS Polysilicon Vibrating Ring Gyroscope," IEEE Journal of Microelectromechanical Systems, vol. 10, June 2001, pp. 169-179.

[9] Marek, Jiri. "MEMS for automotive and consumer electronics." *Solid-State Circuits Conference Digest of Technical Papers (ISSCC), 2010 IEEE International*. IEEE, 2010.

[10] Next Generation of MEMS gyroscopes and inertial combo sensors from SensorDynamics, [online]: http://www.i-micronews.com/news/Generation-MEMS-gyroscopes-inertial-combo-sensors-SensorDyn,6375.html

[11] H. Johari and F. Ayazi, "High Frequency Capacitive Disk Gyroscopes in (100) and (111) Silicon," Proc. 20th IEEE International Conf. on Micro Electro Mechanical Systems (MEMS 2007), Kobe, Japan, Jan. 2007, pp. 47-50.

References

[12] W. K. Sung, M. Dalal, and F. Ayazi, "A Mode-Matched 0.9 MHz Single Proof-Mass Dual-Axis Gyroscope," Tech. Digest of the 16th International Conference on Solid-State Sensors, Actuators and Microsystems (TRANSDUCERS'11), Beijing, China, June 2011, pp. 2821-2824.

[13] F. Ayazi, "Multi-DOF Inertial MEMS: From Gaming to Dead Reckoning," *Invited Paper*, Tech. Digest of the 16th International Conference on Solid-State Sensors, Actuators and Microsystems (TRANSDUCERS'11), Beijing, China, June 2011, pp. 2805-2808.

[14] Lynch, D. "Vibratory gyro analysis by the method of averaging." *Proc. 2nd St. Petersburg Conf. on Gyroscopic Technology and Navigation, St. Petersburg*. 1995.

[15] R. Tabrizian, M. Hodjat-Shamami, and F. Ayazi. "High-Frequency AlN-on-Silicon Resonant Square Gyroscopes." IEEE Journal of Microelectromechanical Systems, Vol. 22, Issue 5, October 2013, pp. 1007-1009.

[16] Bryan, G. H. "On the beats in the vibrations of a revolving cylinder or bell." *Proceedings of the Cambridge Philosophical Society*. Vol. 7. No. 1. 1890.

[17] J. A. Gregory, "Characterization, Control and Compensation of MEMS Rate and Rate-Integrating Gyroscopes", Doctoral Dissertation, University of Michigan, 2012

[18] Alexander A. Trusov, Igor P. Prikhodko, Sergei A. Zotov, Andrei M. Shkel, "Low-Dissipation Silicon MEMS Tuning Fork Gyroscopes for Rate and Whole Angle Measurements," IEEE Sensors Journal, vol. 11, no. 11, pp. 2763-2770, November 2011.

[19] L. Sorenson, P. Shao, and F. Ayazi, "Effect of thickness anisotropy on degenerate modes in oxide micro-hemispherical shell resonators" IEEE International Conference on Micro Electro Mechanical Systems (MEMS 2013), Taibei, Taiwan, Jan. 2013, pp. 169-172

IEEE

SENSORS 2013

Tutorials: November 3, 2013 Conference: November 4-6, 2013

Sponsored by the IEEE Sensors Council, www.ieee-sensors.org

Georgia Institute of Technology

IMEMS

Qualtré